NATIONAL ADVISORY COMMITTEE FOR AERONAUTICS

TECHNICAL NOTE 4088

PRACTICAL SOLUTION OF PLASTIC DEFORMATION PROBLEMS IN ELASTIC-PLASTIC RANGE

By A. Mendelson and S. S. Manson

Lewis Flight Propulsion Laboratory
Cleveland, Ohio

Washington
September 1957

NATIONAL ADVISORY COMMITTEE FOR AERONAUTICS

TECHNICAL NOTE 4088

PRACTICAL SOLUTION OF PLASTIC DEFORMATION PROBLEMS IN ELASTIC-PLASTIC RANGE

By A. Mendelson and S. S. Manson

SUMMARY

A practical method for solving plastic deformation problems in the elastic-plastic range is presented. The method is one of successive approximations and is illustrated by four examples which include a flat plate with temperature distribution across the width, a thin shell with axial temperature distribution, a solid cylinder with radial temperature distribution, and a rotating disk with radial temperature distribution.

INTRODUCTION

The calculation of stresses in structural components in which plastic flow is considered is currently of great interest in order to take full advantage of the load-carrying capacity of available materials. Little attention, however, has been directed at providing simple, general methods which can be applied by the engineer toward the solution of practical problems. This report presents such a method and its applications to several problems of current interest. Although use is made of a technique arising in the theory of integral equations, no knowledge of integral equations is required, and the mathematics involved is well within the scope of the practicing engineer.

The method, which is one of successive integrations, is illustrated for four different thermal stress problems which include the flat plate with temperature variation along the width, the thin cylindrical shell with axial temperature distribution, the solid cylinder with radial temperature distribution, and the rotating disk with radial temperature distribution. The techniques illustrated are not, however, limited to thermal stress problems. The first three problems considered involve small plastic strains, that is, on the same order of magnitude as the elastic strains. The fourth problem involves strains on the order of 1 percent. The deformation theory of plasticity with the Von Mises yield condition is used. Other yield conditions, however, could be used.

METHOD

The determination of stresses and strains in a body consists of combining the equations of equilibrium and compatibility with the "stress-strain" relation and integrating the resulting equations. For both elastic and plastic problems the same equations result for equilibrium and compatibility; the difference in the two cases consists of the stress-strain relation. In the elastic case a linear relation applies between stress and strain, thus resulting in linear differential equations which can be solved by standard methods. The occurrence of plastic flow greatly complicates the problem by introducing a nonlinear stress-strain relation resulting in a nonlinear differential equation for which direct solutions may be difficult or impossible to obtain. The present report demonstrates a relatively simple method for obtaining approximate solutions to the resulting nonlinear differential equations whereby the equations are first converted to nonlinear integral equations and then solved by the established mathematical technique of successive integrations.

The principle underlying the successive integration method of the solution of plastic flow problems can best be illustrated by an example which is treated in greater detail in the section EXAMPLES. For a flat plate subject to a temperature variation along the chord $T = 600(y^2 - 1/3) + T_0$ the total strain ϵ due to stress is given by

$$\epsilon = -0.00570(y^2 - 1/3) + \int_0^1 \epsilon_{ep}\, dy \qquad (1)$$

where the plastic strain ϵ_{ep} is a function of the total strain ϵ (fig. 1). (All symbols are defined in appendix A.)

A convenient method for solving equation (1) is to approach the solution in successive steps by organizing the computations so that the bothersome nonlinear terms are treated not as unknowns but as known quantities determinable from a previous iteration. For example, as a zeroth approximation, let it be assumed that $\epsilon_{ep} = 0$ for all values of y. Then equation (1) permits direct computation of ϵ for all values of y. Once the total strain ϵ is determined, the plastic component of the strain ϵ_{ep} may be obtained by inspection of the stress-strain curve (fig. 1) or by simple computation. It is thus possible in the next computation to include the ϵ_{ep} terms as determined from the first computation, and thus somewhat more accurate values of ϵ can be obtained. These in turn lead to more accurate values of ϵ_{ep}, and the process is repeated, each time with the plastic strain terms determined in the previous iteration being treated as known quantities. When successive iterations lead to no change in ϵ or ϵ_{ep}, it manifestly makes no difference

whether the ϵ_{ep} terms apply to the current or previous iteration. Equation (1) is now satisfied to the desired degree of accuracy, and the correct solution is therefore obtained.

The simple example of the flat plate just illustrated involves uniaxial stress, hence it is possible to determine directly plastic strain once the total strains are known. In most cases of practical interest the stresses are biaxial or triaxial, and the formal procedure for carrying through the computations can be illustrated by referring to the case of the long solid cylinder with radial temperature distribution, which is also treated in greater detail in the section Long Solid Cylinder. By manipulating the equilibrium and compatibility equations and the stress-strain relations, expressions for the total strains in three principal directions are derived in integral equation forms of the type

$$\epsilon_r = f(r) + \int_0^r g(r, \epsilon_r, \epsilon_\theta, \epsilon_z, \epsilon_{rp}, \epsilon_{\theta p})dr \qquad (2)$$

with similar expressions for ϵ_θ and ϵ_z. If an attempt is made to write a direct relation between the elastic and plastic strains derived from plasticity laws and this relation is substituted in equation (2), complicated nonlinear integral equations result which do not readily admit solution. These complications can again be avoided by the process of successive integrations. The zeroth approximation for the total strains ϵ_r, ϵ_θ, and ϵ_z is determined by neglecting the integral term, thereby ϵ_r is made equal to $f(r)$ with similar assumptions for ϵ_θ and ϵ_z. For these values of total strains the plastic strains are determined as will be discussed presently. These values of plastic strains are now treated as known values and substituted into equation (2) to determine first approximations to total strains ϵ_r, ϵ_θ, and ϵ_z from which new approximations to the plastic strains can be determined. The process is repeated as many times as necessary until successive approximations show sufficiently little change in total or plastic strains to permit being considered as converged to the correct solution.

It may be noted that the method of successive integrations is not completely new in application to plastic flow problems. Ilyushin's treatment of the thin shell (ref. 1) is essentially a successive integration process similar to that discussed in this report. Although he regarded the successive iterations as a series of artificial elastic problems, the mechanics of the computations are identical to those resulting when the problem is treated strictly in its mathematical sense of successive integrations of a nonlinear integral equation. In the present paper the thin shell problem is treated without the restrictions imposed by Ilyushin of linear strain-hardening and of complete incompressibility in the elastic-plastic range.

In order to determine new values for the plastic strains ϵ_{rp} and $\epsilon_{\theta p}$ from the values of the total strains ϵ_r, ϵ_θ, and ϵ_z as calculated by equations such as equation (2), a stress-strain relation for biaxial or triaxial stresses in the elastic-plastic range is needed. It will be seen that the validity of the method does not depend on the precise form of the stress-strain relations, but for illustrative purposes it was necessary to select specific relations. The relations of the deformation theory of plasticity were therefore used. Appendix B shows that by introducing the concept of equivalent total strain, the plastic strains can be computed from the total strains in a simple fashion. Thus, the equivalent total strain ϵ_{et} may be defined as follows:

$$\epsilon_{et} \equiv \frac{\sqrt{2}}{3}\sqrt{(\epsilon_r - \epsilon_\theta)^2 + (\epsilon_r - \epsilon_z)^2 + (\epsilon_\theta - \epsilon_z)^2} \tag{3}$$

Then the plastic strains are given by:

$$\left.\begin{aligned} \epsilon_{rp} &= \frac{1}{3}\frac{\epsilon_{ep}}{\epsilon_{et}}(2\epsilon_r - \epsilon_\theta - \epsilon_z) \\ \epsilon_{\theta p} &= \frac{1}{3}\frac{\epsilon_{ep}}{\epsilon_{et}}(2\epsilon_\theta - \epsilon_r - \epsilon_z) \end{aligned}\right\} \tag{4}$$

where ϵ_{ep} is the equivalent plastic strain as shown on the uniaxial tensile curve of figure 1. Furthermore, it is shown in appendix B that the equivalent total strain ϵ_{et} can be written as follows:

$$\epsilon_{et} = \frac{2(1 + \nu)}{3}\frac{\sigma_e}{E} + \epsilon_{ep} \tag{5}$$

where the equivalent stress σ_e is the ordinate of the uniaxial stress-strain curve as shown in figure 1. Since, for a given value of ϵ_{ep}, σ_e can be directly determined from this stress-strain curve, equation (5) permits the direct construction of a curve of ϵ_{et} against ϵ_{ep} as shown in figure 2. The computation of the plastic strains thus becomes very simple. For a given set of values of total strain, ϵ_{et} is computed from equation (3). For this value of ϵ_{et}, ϵ_{ep} is read from figure 2, and ϵ_{rp} and $\epsilon_{\theta p}$ are then computed from equations (4). These values of ϵ_{rp} and $\epsilon_{\theta p}$ are substituted into equations such as equation (2) to obtain new values for the total strains ϵ_r, ϵ_θ, and ϵ_z.

In some cases it is possible to expedite the calculation of plastic strains for known values of total strains by preparing charts in advance of the calculation. Use of such charts will be illustrated in the examples for the thin circular shell.

The question arises as to whether the process is always convergent to the correct solution, or whether it is possible at some point for successive solutions to become worse than earlier ones, thus they could lead ultimately to meaningless results. In all the cases treated in this report it can be shown that the functions appearing in the integral equations satisfy the conditions necessary for the convergence of the process (ref. 2); hence, the correct solution must result if a sufficiently large number of iterations are performed. However, for some problems the rate of convergence may be very slow, and a large number of iterations may be required to obtain a solution of the desired accuracy. Two devices may be employed to expedite the convergence. It appears reasonable to assume that the closer the initially assumed solution is to the correct solution, the fewer the number of iterations that will be required before convergence will result. Hence, any knowledge or insight possessed by the investigator should be used to estimate the zeroth approximation, rather than obtaining it by assuming all plastic strains to be zero. Solution to related problems, solutions by other approximate or simpler methods, approximate measurements, physical intuition, or other expedients accessible to the investigator may all be used to good advantage. For example, some problems may be formulated in which the stresses will evidently change little because of plastic flow, and the strains will have to assume whatever values are necessary to permit these stresses to be generated. (This is a contrasting case to that of thermally induced stress in which the strains govern and take on approximately their elastically computed values, and the stresses adjust accordingly.) In such cases it may be better to start with an assumed initial stress distribution, compute the corresponding elastic strains from the stress-strain relation, and proceed with successive integrations based on this initial strain distribution.

Even when no insight into the correct solution is available, convergence may still be expedited by noting essentially the rate at which successive iterations change the strain distribution. A formal technique using this concept is illustrated in this report in connection with the rotating disk. It also should be noted that, if high-speed computing machinery is used, the number of successive approximations required for convergence becomes of lesser importance. The method will now be illustrated for four different problems.

EXAMPLES

Thin Flat Plate

As a first example, consider the simple uniaxial case of a thin infinite plate of width $2c$ with a temperature distribution $T(y)$ across the width. Under these conditions, the only nonzero stress is $\sigma_x = \sigma_x(y)$. As in the usual theory of bending, it is assumed that plane sections remain plane. This requires that

$$\epsilon_x = a + by \tag{6}$$

where a and b are constants to be determined.

The stress-strain relation is

$$\epsilon_x = \frac{1}{E}\sigma_x + \alpha T + \epsilon_{xp} \tag{7}$$

The boundary conditions require that

$$\left.\begin{aligned} \int_{-c}^{c} \sigma_x \, dy &= 0 \\ \int_{-c}^{c} \sigma_x y \, dy &= 0 \end{aligned}\right\} \tag{8}$$

Combining equations (6), (7), and (8) gives

$$\left.\begin{aligned} \int_{-c}^{c} E(a + by - \alpha T - \epsilon_{xp}) dy &= 0 \\ \text{and} \qquad \int_{-c}^{c} E(a + by - \alpha T - \epsilon_{xp}) y \, dy &= 0 \end{aligned}\right\} \tag{9}$$

If E is constant, equations (9) give

$$\left.\begin{aligned} a &= \frac{1}{2c}\int_{-c}^{c} \alpha T \, dy + \frac{1}{2c}\int_{-c}^{c} \epsilon_{xp} \, dy \\ b &= \frac{3}{2c^3}\int_{-c}^{c} \alpha T y \, dy + \frac{3}{2c^3}\int_{-c}^{c} \epsilon_{xp} y \, dy \end{aligned}\right\} \tag{10}$$

Also, in this case

$$\left.\begin{aligned} \epsilon_{xp} &= \epsilon_{ep} \\ \sigma_e &= \sigma_x \end{aligned}\right\} \tag{11}$$

Equations (6) can now be written as follows:

$$\epsilon_x - \alpha T = \epsilon = \frac{1}{2c}\int_{-c}^{c} \alpha T \, dy + \frac{3y}{2c^3}\int_{-c}^{c} \alpha T y \, dy - \alpha T + \frac{1}{2c}\int_{-c}^{c} \epsilon_{ep} \, dy + \frac{3y}{2c^3}\int_{-c}^{c} \epsilon_{ep} y \, dy \tag{12}$$

As a specific example, let

$$T = 600(y^2 - 1/3) + T_0$$

$$E = 28\times10^6$$

$$c = 1$$

$$\alpha = 9.5\times10^{-6}$$

The stress-strain curve for the material is given by figure 1. Because of symmetry only half the plate between 0 and 1 need be considered. Equation (12) becomes

$$\epsilon_x - \alpha T = \epsilon = -0.00570(y^2 - 1/3) + \int_0^1 \epsilon_{ep} \, dy \tag{13}$$

Equation (13) is now solved by successive approximations by using the stress-strain curve (fig. 1). For the zeroth approximation to the total strains it is assumed that the total strains do not change much from those computed "elastically" and, therefore, that ϵ_{ep} is everywhere zero. The integral in equation (13) thus vanishes, and the strains are computed. This is the elastically computed strain distribution. With this strain distribution, a first approximation to the plastic strains ϵ_{ep} is obtained directly from the stress-strain curve (fig. 1). The integral in equation (13) is now evaluated, and a first approximation to the total strains is obtained. With this first approximation, a second approximation to the plastic strains is obtained from the stress-strain curve. The process is repeated until the desired convergence is obtained. The integral in equation (13) was evaluated simply by the trapezoidal rule. More accurate evaluation, for example, by Simpson's rule, can be made if desired.

The computations for this problem are shown in table I, and the results are plotted in figure 3. The stresses, which are not shown in table I, can be read directly from the stress-strain curve once the strains are computed. These calculations show that the first approximation is sufficiently accurate and that the total strains are not much different from those computed elastically. This last result explains the fast convergence of this method for this problem.

If the modulus of elasticity E is not constant, no additional difficulty is added. Solution of equation (9) gives, for a and b:

$$\left.\begin{aligned} a = {} & A_1 \int_{-c}^{c} E\alpha T \, dy + A_1 \int_{-c}^{c} E\epsilon_{xp} \, dy - \\ & A_2 \int_{-c}^{c} E\alpha T y \, dy - A_2 \int_{-c}^{c} E\epsilon_{xp} y \, dy \\ b = {} & -A_2 \int_{-c}^{c} E\alpha T \, dy - A_2 \int_{-c}^{c} E\epsilon_{xp} y \, dy + \\ & A_3 \int_{-c}^{c} E\alpha T y \, dy + A_3 \int_{-c}^{c} E\epsilon_{xp} y \, dy \end{aligned}\right\} \tag{14}$$

where A_1, A_2, and A_3 are numbers which are determined once and for all for a particular problem from the known variation of E with temperature:

$$\left.\begin{aligned} A_1 &= \frac{\int_{-c}^{c} Ey^2 \, dy}{\int_{-c}^{c} E \, dy \int_{-c}^{c} Ey^2 \, dy - \left(\int_{-c}^{c} Ey \, dy \right)^2} \\ A_2 &= \frac{\int_{-c}^{c} Ey \, dy}{\int_{-c}^{c} E \, dy \int_{-c}^{c} Ey^2 \, dy - \left(\int_{-c}^{c} Ey \, dy \right)^2} \\ A_3 &= \frac{\int_{-c}^{c} E \, dy}{\int_{-c}^{c} E \, dy \int_{-c}^{c} Ey^2 \, dy - \left(\int_{-c}^{c} Ey \, dy \right)^2} \end{aligned}\right\} \tag{15}$$

By using these values for a and b the solution is obtained by successive approximations as before. Of course, a different stress-strain curve must be used at every station and is dependent on the temperature of that station.

Thin Circular Shell

The second example considered is that of a thin circular shell with axial temperature gradient. The equations for the total strains, presented in appendix C, are

$$\left.\begin{aligned} \epsilon_x &= \nu \frac{w}{R} - \frac{1}{l^2}\frac{d^2w}{dx^2} z + (1+\nu)\alpha T + \frac{1}{H}\int_{-H/2}^{H/2} (\epsilon_{xp} + \nu\epsilon_{\theta p})dz \\ \epsilon_\theta &= -\frac{w}{R} \\ \epsilon_z &= -\frac{\nu}{1-\nu}(\epsilon_x + \epsilon_\theta) + \frac{1+\nu}{1-\nu}\alpha T - \frac{1-2\nu}{1-\nu}(\epsilon_{xp} + \epsilon_{\theta p}) \end{aligned}\right\} \quad (16)$$

where w is the solution of

$$\frac{d^4w}{dx^4} + 4w = -4R\alpha T - \frac{d^2P}{dx^2} - Q \quad (17)$$

and is given by

$$w = c_1 \cos x \cosh x + c_2 \cos x \sinh x + c_3 \sin x \cosh x + c_4 \sin x \sinh x - 4R\int_0^x \alpha T(\xi)G(x-\xi)d\xi - \int_0^x P(\xi)\frac{d^2G(x-\xi)}{dx^2}d\xi - \int_0^x Q(\xi)G(x-\xi)d\xi \quad (18)$$

and

$$\left.\begin{aligned} G(x - \xi) &= \frac{1}{4}\left[\sin(x - \xi)\cosh(x - \xi) - \cos(x - \xi)\sinh(x - \xi)\right] \\ P &= \frac{12\ell^2}{H^3}\int_{-H/2}^{H/2} (\epsilon_{xp} + \nu\epsilon_{\theta p})z\, dz \\ Q &= \frac{4R}{H}\int_{-H/2}^{H/2} \epsilon_{\theta p}\, dz \end{aligned}\right\} \quad (19)$$

The term $G(x - \xi)$ is the Green's function for this problem. Substitution verifies that equation (18) is a solution of equation (17).

The solution to the problem is now obtained by successive approximations starting with the assumption that ϵ_{xp} and $\epsilon_{\theta p}$ are zero. A zeroth approximation to the total strains can thus be obtained from equations (16) and (18). With these values of total strain, first approximations to the plastic strains ϵ_{xp} and $\epsilon_{\theta p}$ can be readily obtained as will be shown. These first approximations to the plastic strains are substituted in equations (16), (18), and (19), and first approximations to the total strains ϵ_x, ϵ_θ, and ϵ_z are obtained. The process is repeated as many times as necessary to give the desired convergence. For every successive approximation the constants c_1 to c_4 appearing in equation (18) must be evaluated in order to satisfy the boundary conditions.

To obtain the plastic strains ϵ_{xp} and $\epsilon_{\theta p}$ once the total strains ϵ_x, ϵ_θ, and ϵ_z have been determined for any iteration, the stress-strain curve and equations (3) and (4) are used. In order to facilitate the computation of ϵ_{xp} and $\epsilon_{\theta p}$, a cross plot is made of the stress-strain curve as is shown in figure 2 by means of equation (5) as previously explained. The process for obtaining the plastic strains ϵ_{xp} and $\epsilon_{\theta p}$ from the total strains now becomes relatively simple. For a given set of strains ϵ_x, ϵ_θ, and ϵ_z, the equivalent total strain ϵ_{et} is computed by equation (3). For this value of ϵ_{et}, ϵ_{ep} is obtained from figure 2, and ϵ_{xp} and $\epsilon_{\theta p}$ are computed by equations (4). It should be noted that the curve in figure 2 is very close to a straight line. The equation of the "best fit" straight line was therefore used in some of the computations. Representation of the curve by a functional relation is particularly useful if a given problem is set up for automatic machine computation.

As an alternate procedure, the plastic strains ϵ_{xp} and $\epsilon_{\theta p}$ can be obtained directly from the total strains ϵ_x and ϵ_θ by means of a parametric family of curves as shown in figure 4. For a given pair of values of $\epsilon_x - \alpha T$ and $\epsilon_\theta - \alpha T$, the plastic strains are read directly from these curves. Figure 4 was obtained from the stress-strain curve (fig. 1) as explained in appendix D. This procedure avoids the necessity of computing ϵ_z from the last part of equations (16), ϵ_{et} from equation (3), and ϵ_{rp} and $\epsilon_{\theta p}$ from equations (4). However, obtaining a set of curves such as those in figure 5 involves a considerable amount of labor, and it is usually not worthwhile to make such a chart unless several similar computations are to be made using the same stress-strain curve.

It is to be noted that the stresses can be computed at any step of the calculation by the stress-strain relations:

$$\left.\begin{aligned} \sigma_x &= \frac{E}{1 - \nu^2}\left[\epsilon_x - \alpha T - \epsilon_{xp} + \nu(\epsilon_\theta - \alpha T - \epsilon_{\theta p})\right] \\ \sigma_\theta &= \frac{E}{1 - \nu^2}\left[\epsilon_\theta - \alpha T - \epsilon_{\theta p} + \nu(\epsilon_x - \alpha T - \epsilon_{xp})\right] \end{aligned}\right\} \tag{20}$$

The solution will now be illustrated for a specific problem. Consider a thin circular shell with the following geometric and physical properties:

$L = 48$ in.

$R = 12$ in.

$H = 2$ in.

$\nu = 0.3$

$$l = \sqrt[4]{\frac{R^2H^2}{3(1 - \nu^2)}} = 3.81 \text{ in.}$$

$E = 28 \times 10^6$ lb/sq in.

$\alpha = 9.5 \times 10^{-6}\ {}^\circ F^{-1}$

$T = 2.21x^2$ (corresponds to 350° F rise from one end of shell to other)

$0 \leqslant x \leqslant 12.6$

With the stress-strain curve of figure 1 and the following boundary conditions

$$w(0) = w'(0) = w(12.6) = w'(12.6) = 0 \tag{21}$$

the functions P and Q become

$$\left.\begin{aligned} P &= 21.8 \int_{-1}^{1} (\epsilon_{xp} + 0.3\epsilon_{\theta p})z \, dz \\ Q &= 24 \int_{-1}^{1} \epsilon_{\theta p} \, dz \end{aligned}\right\} \tag{22}$$

From the first two boundary conditions,

$$c_1 = 0$$

$$c_2 = -c_3$$

Also, the first integral on the right side of equation (18) becomes

$$4R \int_0^x \alpha T(\xi)G(x - \xi)d\xi = 0.000252x^2 + 0.000252 \sin x \sinh x$$

Equation (18) now becomes

$$w(x) = c_2(\cos x \sinh x - \sin x \cosh x) + c_4 \sin x \sinh x - 0.000252x^2 - I_1(x) - I_2(x) \tag{23}$$

where

$$\left.\begin{aligned} I_1 &\equiv \int_0^x Q(\xi)G(x - \xi)d\xi \\ I_2 &\equiv \int_0^x P(\xi) \frac{d^2G(x - \xi)}{dx^2} \, d\xi \end{aligned}\right\} \tag{24}$$

For the zeroth approximation, it is assumed that ϵ_{xp} and $\epsilon_{\theta p}$ and, therefore, I_1 and I_2 are zero. The function $w(x)$ is calculated from equation (23) with the constants c_2 and c_4 determined from the last two boundary conditions (eq. (21)). The strains ϵ_x, ϵ_θ, and ϵ_z are

then computed from equations (16). First approximations to ϵ_{xp} and $\epsilon_{\theta p}$ are now obtained either directly from figure 5 or by computing ϵ_{et} from equation (3), reading ϵ_{ep} from figure 2, and calculating ϵ_{xp} and $\epsilon_{\theta p}$ from equations (4). For this particular example figure 5 was used. For the two examples to be discussed subsequently, equations (3) and (4), in conjunction with figure 2, were used. With these values of ϵ_{xp} and $\epsilon_{\theta p}$, P and Q are computed from equations (22), w from equations (23) and (24), and new values of ϵ_x, ϵ_θ, and ϵ_z from equations (16). The process is repeated until convergence is obtained.

Wherever derivatives of w are needed such as in the first part of equations (16) and in equation (21), the following relations are useful:

$$\left.\begin{aligned}
\frac{dI_1}{dx} &= \int_0^x Q(\xi)\,\frac{dG(x-\xi)}{dx}\,d\xi \\
\frac{dI_2}{dx} &= \int_0^x P(\xi)\,\frac{d^3G(x-\xi)}{dx^3}\,d\xi \\
\frac{d^2I_1}{dx^2} &= \int_0^x Q(\xi)\,\frac{d^2G(x-\xi)}{dx^2}\,d\xi \\
\frac{d^2I_2}{dx^2} &= -4\int_0^x P(\xi)G(x-\xi)\,d\xi + P(x)
\end{aligned}\right\} \tag{25}$$

and

$$\left.\begin{aligned}
\frac{dG(x-\xi)}{dx} &= \frac{1}{2}\sin(x-\xi)\sinh(x-\xi) \\
\frac{d^2G(x-\xi)}{dx^2} &= \frac{1}{2}\left[\sin(x-\xi)\cosh(x-\xi) + \cos(x-\xi)\sinh(x-\xi)\right] \\
\frac{d^3G(x-\xi)}{dx^3} &= \cos(x-\xi)\cosh(x-\xi)
\end{aligned}\right\} \tag{26}$$

The integrals in equations (24) and (25) were evaluated using the trapezoidal rule. Thus, in order to evaluate the integrals at a station $x = x_j$,

$$\int_0^{x_j} f(\xi)F(x_j - \xi)d\xi \cong \Delta x\left(\frac{1}{2} f_0F_j + f_1F_{j-1} + f_2F_{j-2} + \ldots + f_{j-1}F_1 + \frac{1}{2} f_jF_0\right) \tag{27}$$

The results for this problem are shown in figure 5. An abbreviated calculation setup for one of the successive approximations is shown in table I(b). As many as seven successive approximations were carried out as shown in the figures, and the differences between the seventh and the fourth approximations are very small. From an engineering viewpoint the first approximation is actually sufficient. Again, the total strains did not change very much, which explains the relatively rapid convergence.

Long Solid Cylinder

The plane strain problem of a long solid cylinder with a radial temperature distribution is considered next. Appendix E shows that if the modulus of elasticity E is assumed constant, the total strains are given by

$$\left.\begin{aligned}
\epsilon_\theta &= \frac{1+\nu}{1-\nu}\frac{1}{r^2}\int_0^r \alpha T r\,dr + \frac{1-2\nu}{2(1-\nu)}\frac{1}{r^2}\int_0^r (\epsilon_{rp} + \epsilon_{\theta p})r\,dr + \\
&\quad \frac{1-2\nu}{2(1-\nu)}\int_0^r \frac{\epsilon_{rp} - \epsilon_{\theta p}}{r}\,dr + C_1 \\
\epsilon_r &= -\epsilon_\theta + \frac{1+\nu}{1-\nu}\alpha T + \frac{1-2\nu}{1-\nu}\epsilon_{rp} + \frac{1-2\nu}{1-\nu}\int_0^r \frac{\epsilon_{rp} - \epsilon_{\theta p}}{r}\,dr + 2C_1 \\
\epsilon_z &= \frac{2}{R^2}\left[\int_0^R \alpha T r\,dr - \int_0^R (\epsilon_{rp} + \epsilon_{\theta p})r\,dr\right] \\
C_1 &= \frac{1-3\nu}{1-\nu}\frac{1}{R^2}\int_0^R \alpha T r\,dr - \frac{1-2\nu}{2(1-\nu)}\int_0^R \frac{\epsilon_{rp} - \epsilon_{\theta p}}{r}\,dr + \\
&\quad \frac{1}{2(1-\nu)}\frac{1}{R^2}\int_0^R (\epsilon_{rp} + \epsilon_{\theta p})r\,dr
\end{aligned}\right\} \tag{28}$$

Equations (28) are now solved by successive approximations as for the previous examples. The zeroth approximation to the total strains is obtained from equations (28) by assuming that ϵ_{rp} and $\epsilon_{\theta p}$ are zero. The total equivalent strain is then computed by equation (3), the equivalent plastic strain is read from figure 2, and first approximations to ϵ_{rp} and $\epsilon_{\theta p}$ are obtained from equations (4). These values of ϵ_{rp} and $\epsilon_{\theta p}$ are substituted into equations (28), and new approximations are obtained for ϵ_r, ϵ_θ, and ϵ_z. The process is then repeated as many times as necessary to obtain the desired degree of convergence. The stresses can be computed at any time from the general stress-strain relations:

$$\left.\begin{aligned}
\sigma_r &= \lambda(\epsilon_r + \epsilon_\theta + \epsilon_z - 3\alpha T) + 2G(\epsilon_r - \alpha T - \epsilon_{rp}) \\
\sigma_\theta &= \lambda(\epsilon_r + \epsilon_\theta + \epsilon_z - 3\alpha T) + 2G(\epsilon_\theta - \alpha T - \epsilon_{\theta p}) \\
\sigma_z &= \lambda(\epsilon_r + \epsilon_\theta + \epsilon_z - 3\alpha T) + 2G(\epsilon_z - \alpha T + \epsilon_{rp} + \epsilon_{\theta p})
\end{aligned}\right\} \quad (29)$$

The above calculations have been carried out for a 1-inch-radius cylinder with a temperature gradient as shown in figure 6 and by using the stress-strain curve of figure 1. The computations are shown in table I(c) for one iteration, and the results are plotted in figure 7. Little difference occurred between the fourth and fifth approximations.

Rotating Disk with Temperature Gradient

As a final example the plane stress problem of a parallel-sided rotating disk with a radial temperature gradient and a constant value of E will be considered. In this problem the strains are considerably

larger than those in the previous examples. The total strains for this case, as shown in appendix F, are given by

$$\left.\begin{aligned}
\epsilon_\theta &= -\frac{1-\nu^2}{E}\frac{\rho\omega^2 r^2}{8} + \frac{1+\nu}{r^2}\int_0^r \alpha T r\,dr + \frac{1-\nu}{2}\int_0^r \frac{\epsilon_{rp}-\epsilon_{\theta p}}{r}\,dr + \\
&\quad \frac{1+\nu}{2r^2}\int_0^r (\epsilon_{rp}+\epsilon_{\theta p})r\,dr + \frac{C_3}{2} \\
\epsilon_r &= -\epsilon_\theta - \frac{1-\nu^2}{E}\frac{\rho\omega^2 r^2}{2} + (1+\nu)\alpha T + \epsilon_{rp} + \nu\epsilon_{\theta p} + \\
&\quad (1-\nu)\int_0^r \frac{\epsilon_{rp}-\epsilon_{\theta p}}{r}\,dr + C_3 \\
\epsilon_z &= -\frac{\nu}{1-\nu}(\epsilon_r+\epsilon_\theta) + \frac{1+\nu}{1-\nu}\alpha T - \frac{1-2\nu}{1-\nu}(\epsilon_{rp}+\epsilon_{\theta p}) \\
C_3 &= 2(1-\nu)\left[\frac{\sigma_R}{E} + \frac{3+\nu}{8E}\rho\omega^2 R^2 + \frac{1}{R^2}\int_0^R \alpha T r\,dr - \frac{1}{2}\int_0^R \frac{\epsilon_{rp}-\epsilon_{\theta p}}{r}\,dr + \right. \\
&\quad \left. \frac{1}{2R^2}\int_0^R (\epsilon_{rp}+\epsilon_{\theta p})r\,dr\right]
\end{aligned}\right\} \tag{30}$$

The solution to this problem is obtained by successive approximation exactly as in the previous example for the solid cylinder. By starting with assumed values of ϵ_{rp} and $\epsilon_{\theta p}$ equal to zero, ϵ_r, ϵ_θ, and ϵ_z are computed from equations (30), ϵ_{et} from equation (3), ϵ_{ep} from figure 2, and ϵ_{rp} and $\epsilon_{\theta p}$ from equations (4). New values of ϵ_r, ϵ_θ, and ϵ_z are now obtained from equations (30), and the process is repeated.

A solution was obtained in this manner for a 10-inch-diameter disk with a temperature gradient as shown in figure 8. The value of $\rho\omega^2$ was taken as 1500, and the stress-strain curve of figure 1 was used. The computations for one iteration are shown in table I(d), and the results

are plotted in figure 9. In this problem, the strains are relatively large, with the maximum equivalent strain close to 1 percent. A straightforward application of this method therefore requires approximately 40 iterations in order to obtain accurate results. However, the convergence can be greatly increased by performing three or four iterations, taking the differences between successive iterations for the various strains, and extrapolating to a zero difference as shown in figure 10. A root-mean-square line is drawn, and the intercept at zero $\Delta\epsilon$ is obtained. This furnishes a new starting estimate. Three or four more successive approximations are carried out, and another similar extrapolation is made. This technique reduced the number of successive approximations for this problem from about 40 to about 12.

This same problem was solved by the trial-and-error method of reference 3. The results obtained were almost identical to those obtained herein as can be seen in figure 9.

DISCUSSION

The speed of convergence of this method depends primarily on two factors: the amount of plastic flow occurring, and the number of stations taken in the plastic region. For small plastic strains convergence will be relatively fast. Similarly, for a small number of stations in the plastic region relatively few iterations are needed. If the number of stations is increased, more iterations are needed for convergence to occur. Thus, for the case of the thin shell of the second example, doubling the number of stations approximately doubles the number of iterations required for convergence. This is due to the fact that a change in the approximation at one station changes the values at all the other stations, and the more stations there are the longer it takes for all the stations to converge.

Increasing the number of stations therefore increases the labor required for two reasons: the time per iteration goes up, and the number of iterations required increases. Of course, the greater the number of stations used, the greater is the final accuracy attainable. However, good accuracy can be obtained without increasing the labor greatly by following one or both of the following techniques. A calculation is made with a small number of stations to obtain an approximate plastic strain distribution. This strain distribution is then used as a first approximation in a new calculation using more stations. Also, an extrapolation technique such as shown in the rotating disk example can be used to speed up convergence greatly. It should be noted that doubling the number of stations for the thin-shell problem increased the labor greatly, but the maximum stress was changed by only about 2000 pounds per square inch.

An interesting possible application of the results of the method presented herein may be worth further investigation. It has been found that, for thermal stress problems without additional loads, the total strains do not change very much because of the plastic deformation compared to the elastically computed strains and that the first approximation to the stresses is thus usually fairly good. This leads to the possibility of determining semiempirically the plastic thermal stresses in complicated structures for which even the elastic stress distribution cannot be calculated and for which strain measurements cannot readily be made in the plastic region and at high temperatures. A model of the structure can be constructed, and temperatures and temperature gradients can be simulated on a proportionally reduced scale so that no part of the model flows plastically. The total elastic strains under these conditions can usually be readily measured by means of strain gages. The elastic strains can then be extrapolated by simple proportion to those that would exist at the higher temperatures and gradients actually existing in the structure. By assuming that the total strains are then equal to the strains that would exist if the material remained elastic, the plastic strains are computed from equations (3) and (4) and the stress-strain curve, and an estimate of the stresses is obtained from the stress-strain relations such as equations (29). From the examples presented herein, it would seem that the stresses computed in this manner should be accurate enough for many engineering applications.

In many practical problems it is necessary to take into account previous plastic flow that may have taken place. Thus, for example, in a thermal shock experiment, plastic flow may start at some time during the quenching process, and the material may continue to flow plastically as the process continues. A solution must therefore be obtained at various time increments from the start of the quench, and for each time interval the plastic flow that has already occurred up to that time must be taken into account. Treatment of this case is described in detail in appendix G.

Although the method has been presented for four specific thermal stress problems, it is apparent that it is general in nature and can be applied to a large variety of problems for which the solutions of the elasticity equations are available. No implication is intended, however, that this method is necessarily more accurate or faster than other methods that might be used for specific problems. Thus, the example of the rotating disk with temperature gradient can be treated more rapidly by the method of reference 3. The method of this report does, however, provide a uniform simple approach that can be used for many different types of problems. It is not necessary, therefore, to develop special methods and techniques to handle different types of problems.

Finally, it should be pointed out that, although for uniformity and simplicity the method has been set up by using the equations for total

strains (e.g., eq. (2)), it may be desirable in some cases to deal with the equations for stress which can be put in a similar form. Upon determining σ_r, σ_θ, and σ_z for $\epsilon_{rp} = \epsilon_{\theta p} = 0$ (i.e., the elastic stresses), the elastic total strains can be computed by Hooke's Law. For these total strains the plastic components are evaluated as described earlier, and a first iteration for stress is obtained. Subsequent iterations may follow the same procedure by using as the plastic strains the values determined from the previous iteration. In those cases where it is suspected that the elastic stress distribution is likely to be less affected by the plastic flow than the strain distribution, the plastic strains are determined directly from the stresses and the stress-strain relations as given in appendix B.

SUMMARY OF RESULTS

A method has been presented for solving plastic deformation problems in the elastic-plastic range. The method, one of successive approximations, is illustrated by four examples which included a flat plate, a thin shell, a solid cylinder, and a rotating disk. It was found that for thermal stress problems accurate answers could be obtained with relatively few successive approximations. A technique for speeding up convergence is also shown.

Lewis Flight Propulsion Laboratory
National Advisory Committee for Aeronautics
Cleveland, Ohio, June 20, 1957

APPENDIX A

SYMBOLS

A_1,A_2,A_3	constants
a,b	constants
C_1,C_2,C_3,C_4	integration constants
c	half width of thin plate
c_1,c_2,c_3,c_4	integration constants
E	modulus of elasticity
G	Lamé's constant, $\frac{E}{2(1 + \nu)}$
G(x)	function
H	thickness of thin shell
h	thickness of rotating disk
I_1,I_2	integrals
K_1,K_2	constants (eqs. (B6))
L	length of thin shell
l	characteristic length of thin shell, $\sqrt[4]{\frac{R^2H^2}{3(1 - \nu^2)}}$
P(x)	function
Q(x)	function
R	mean radius of shell, or radius of solid cylinder
r	radial distance to arbitrary point in solid cylinder or rotating disk
T	temperature above arbitrary zero
T_0	arbitrary constant temperature
u	axial displacement of point on middle surface of shell

w	radial displacement of point on middle surface of shell, positive inward
x	ratio of axial coordinate of shell to characteristic length, or axial coordinate of thin plate
y	distance along width of thin plate
z	radial coordinate of thin shell measured from middle surface, positive inward, or axial coordinate of long solid cylinder
α	linear coefficient of thermal expansion
ϵ	conventional strain in tensile test
ϵ_{ep}	equivalent plastic strain
ϵ_{et}	equivalent total strain
$\epsilon_x, \epsilon_\theta, \epsilon_z, \epsilon_r$	strains in x-, θ-, z-, and r-directions, respectively
$\epsilon_{xp}, \epsilon_{\theta p}, \epsilon_{zp}, \epsilon_{rp}$	plastic parts of ϵ_x, ϵ_θ, ϵ_z, and ϵ_r, respectively
θ	tangential coordinate
λ	Lamé's constant, $\frac{\nu E}{(1 + \nu)(1 - 2\nu)}$
ν	Poisson's ratio
ξ	integration variable
ρ	density
σ_e	equivalent stress
$\sigma_x, \sigma_\theta, \sigma_r, \sigma_z$	normal stresses in x-, θ-, r-, and z-directions, respectively
ω	rotational speed of disk

APPENDIX B

CALCULATION OF PLASTIC STRAINS

The deformation theory of plasticity is used with the three usual assumptions that the directions of the principal strains coincide with the directions of the principal stresses, that the ratios of the principal shear strains are equal to the ratios of the principal shear stresses, and that the volume remains constant in the plastic range. These assumptions imply

$$\left.\begin{aligned} \frac{\epsilon_r - \epsilon_\theta}{\sigma_r - \sigma_\theta} = \frac{\epsilon_r - \epsilon_z}{\sigma_r - \sigma_z} = \frac{\epsilon_\theta - \epsilon_z}{\sigma_\theta - \sigma_z} = K_1 \\ \epsilon_{rp} + \epsilon_{\theta p} + \epsilon_{zp} = 0 \end{aligned}\right\} \tag{B1}$$

By substituting the stress-strain relations

$$\left.\begin{aligned} \epsilon_r &= \frac{1}{E}\left[\sigma_r - \nu(\sigma_\theta + \sigma_z)\right] + \epsilon_{rp} + \alpha T \\ \epsilon_\theta &= \frac{1}{E}\left[\sigma_\theta - \nu(\sigma_r + \sigma_z)\right] + \epsilon_{\theta p} + \alpha T \\ \epsilon_z &= \frac{1}{E}\left[\sigma_z - \nu(\sigma_r + \sigma_\theta)\right] + \epsilon_{zp} + \alpha T \end{aligned}\right\} \tag{B2}$$

into the first part of equations (B1), it can also be shown that

$$\frac{\epsilon_{rp} - \epsilon_{\theta p}}{\sigma_r - \sigma_\theta} = \frac{\epsilon_{rp} - \epsilon_{zp}}{\sigma_r - \sigma_z} = \frac{\epsilon_{\theta p} - \epsilon_{zp}}{\sigma_\theta - \sigma_z} = K_2 \tag{B3}$$

where

$$K_1 = K_2 + \frac{1 + \nu}{E} \tag{B4}$$

Define

$$\left.\begin{aligned}
\sigma_e &\equiv \frac{1}{\sqrt{2}} \sqrt{(\sigma_r - \sigma_\theta)^2 + (\sigma_r - \sigma_z)^2 + (\sigma_\theta - \sigma_z)^2} \\
\epsilon_{ep} &\equiv \frac{\sqrt{2}}{3} \sqrt{(\epsilon_{rp} - \epsilon_{\theta p})^2 + (\epsilon_{rp} - \epsilon_{zp})^2 + (\epsilon_{\theta p} - \epsilon_{zp})^2} \\
\epsilon_{ep} &= \frac{2}{\sqrt{3}} \sqrt{\epsilon_{rp}^2 + \epsilon_{rp}\epsilon_{\theta p} + \epsilon_{\theta p}^2} \\
\epsilon_{et} &\equiv \frac{\sqrt{2}}{3} \sqrt{(\epsilon_r - \epsilon_\theta)^2 + (\epsilon_r - \epsilon_z)^2 + (\epsilon_\theta - \epsilon_z)^2}
\end{aligned}\right\} \quad \text{(B5)}$$

Then, by squaring and adding the equations in (B1) and (B3) it readily follows that

$$\left.\begin{aligned}
K_1 &= \frac{3}{2}\frac{\epsilon_{et}}{\sigma_e} \\
K_2 &= \frac{3}{2}\frac{\epsilon_{ep}}{\sigma_e}
\end{aligned}\right\} \quad \text{(B6)}$$

Hence, by the relation between K_1 and K_2 in equation (B4)

$$\epsilon_{et} = \frac{2(1 + \nu)}{3}\frac{\sigma_e}{E} + \epsilon_{ep} \quad (5)$$

The plastic strains can be determined in terms of the total strains by dividing equation (B3) by equations (B1) and applying equations (B6):

$$\frac{\epsilon_{rp} - \epsilon_{\theta p}}{\epsilon_r - \epsilon_\theta} = \frac{\epsilon_{rp} - \epsilon_{zp}}{\epsilon_r - \epsilon_z} = \frac{\epsilon_{\theta p} - \epsilon_{zp}}{\epsilon_\theta - \epsilon_z} = \frac{K_2}{K_1} = \frac{\epsilon_{ep}}{\epsilon_{et}} \quad \text{(B7)}$$

Solving equation (B7) and the incompressibility relation in equations (B1) results in equations (4).

APPENDIX C

EQUATIONS FOR THIN CIRCULAR SHELL

The equilibrium equations for a thin circular cylindrical shell are given in reference 4:

$$\left.\begin{aligned} N_x &= 0 \\ \frac{R}{l^2}\frac{d^2M_x}{dx^2} + N_\theta &= 0 \end{aligned}\right\} \tag{C1}$$

where

$$\left.\begin{aligned} N_x &= \int_{-H/2}^{H/2} \sigma_x \, dz \\ N_\theta &= \int_{-H/2}^{H/2} \sigma_\theta \, dz \\ M_x &= \int_{-H/2}^{H/2} \sigma_x z \, dz \end{aligned}\right\} \tag{C2}$$

The stress-strain relations, including the plastic strains, are

$$\left.\begin{aligned} \sigma_x &= \frac{E}{1-\nu^2}\left[\epsilon_x - \alpha T - \epsilon_{xp} + \nu\left(\epsilon_\theta - \alpha T - \epsilon_{\theta p}\right)\right] \\ \sigma_\theta &= \frac{E}{1-\nu^2}\left[\epsilon_\theta - \alpha T - \epsilon_{\theta p} + \nu\left(\epsilon_x - \alpha T - \epsilon_{xp}\right)\right] \end{aligned}\right\} \tag{C3}$$

The strain displacement relations are

$$\left.\begin{aligned} \epsilon_x &= \frac{du}{l\,dx} - \frac{d^2w}{l^2\,dx^2}z \\ \epsilon_\theta &= -\frac{w}{R} \end{aligned}\right\} \tag{C4}$$

Substituting equations (C4) into (C3) gives

$$\left.\begin{aligned}\sigma_x &= \frac{E}{1-\nu^2}\left[\frac{du}{l\,dx} - \frac{d^2w}{l^2\,dx^2}\,z - \alpha T - \epsilon_{xp} + \nu\left(-\frac{w}{R} - \epsilon_{\theta p} - \alpha T\right)\right] \\ \sigma_\theta &= \frac{E}{1-\nu^2}\left[-\frac{w}{R} - \alpha T - \epsilon_{\theta p} + \nu\left(\frac{du}{l\,dx} - \frac{d^2w}{l^2\,dx^2}\,z - \alpha T - \epsilon_{xp}\right)\right]\end{aligned}\right\} \tag{C5}$$

From the first equation of equations (C1) and (C2),

$$\frac{du}{l\,dx} = \nu\frac{w}{R} + (1+\nu)\alpha T + \frac{1}{H}\int_{-H/2}^{H/2}(\epsilon_{xp} + \nu\epsilon_{\theta p})dz \tag{C6}$$

$$\left.\begin{aligned}N_\theta &= -EH\left(\frac{w}{R} + \frac{1}{H}\int_{-H/2}^{H/2}\epsilon_{\theta p}\,dz + \alpha T\right) \\ M_x &= -\frac{EH^3}{12(1-\nu)^2}\frac{d^2w}{l^2\,dx^2} - \frac{E}{1-\nu^2}\int_{-H/2}^{H/2}(\epsilon_{xp} + \nu\epsilon_{\theta p})z\,dz\end{aligned}\right\} \tag{C7}$$

Substituting equation (C6) into the first of equations (C4) gives

$$\epsilon_x = \nu\frac{w}{R} + (1+\nu)\alpha T + \frac{1}{H}\int_{-H/2}^{H/2}(\epsilon_{xp} + \nu\epsilon_{\theta p})dz - \frac{d^2w}{l^2\,dx^2}\,z \tag{C8}$$

Also, from the second of equations (C1),

$$\frac{d^4w}{dx^4} + 4w = -4R\alpha T - \frac{12l^2}{H^3}\frac{d^2}{dx^2}\int_{-H/2}^{H/2}(\epsilon_{xp} + \nu\epsilon_{\theta p})z\,dz - \frac{4R}{H}\int_{-H/2}^{H/2}\epsilon_{\theta p}\,dz \tag{C9}$$

To obtain ϵ_z, the third stress-strain relation is used:

$$\epsilon_z = \frac{1}{E}\left[\sigma_z - \nu(\sigma_x + \sigma_\theta) + \epsilon_{zp} + \alpha T\right] \tag{C10}$$

Substituting $\sigma_z = 0$ and equations (C3) into equation (C10) gives the third part of equations (16).

APPENDIX D

PLASTIC STRAIN CHARTS

In order to obtain the chart shown in figure 4, the stress-strain relations with $\sigma_z = 0$ are written as follows:

$$\left.\begin{aligned} \epsilon_x - \alpha T &= \frac{1}{E}(\sigma_x - \nu\sigma_\theta) + \epsilon_{xp} \\ \epsilon_\theta - \alpha T &= \frac{1}{E}(\sigma_\theta - \nu\sigma_x) + \epsilon_{\theta p} \end{aligned}\right\} \tag{D1}$$

Also,

$$\left.\begin{aligned} \sigma_x &= \frac{2}{3}\frac{\sigma_e}{\epsilon_{ep}}(2\epsilon_{xp} + \epsilon_{\theta p}) \\ \sigma_\theta &= \frac{2}{3}\frac{\sigma_e}{\epsilon_{ep}}(2\epsilon_{\theta p} + \epsilon_{xp}) \end{aligned}\right\} \tag{D2}$$

Substituting equations (D2) into (D1) gives

$$\left.\begin{aligned} \epsilon_x - \alpha T &= \left[1 + \frac{2}{3}\frac{(2-\nu)}{E}\frac{\sigma_e}{\epsilon_{ep}}\right]\epsilon_{xp} + \frac{2}{3}\frac{(1-2\nu)}{E}\frac{\sigma_e}{\epsilon_{ep}}\epsilon_{\theta p} \\ \epsilon_\theta - \alpha T &= \left[1 + \frac{2}{3}\frac{(2-\nu)}{E}\frac{\sigma_e}{\epsilon_{ep}}\right]\epsilon_{\theta p} + \frac{2}{3}\frac{(1-2\nu)}{E}\frac{\sigma_e}{\epsilon_{ep}}\epsilon_{xp} \end{aligned}\right\} \tag{D3}$$

With the above equations and the stress-strain curve for the material, a two-parameter family of curves can be plotted giving the total strains for any pair of plastic strains ϵ_{xp} and $\epsilon_{\theta p}$. Thus,

(1) An arbitrary convenient value is chosen for $\epsilon_{\theta p}$.

(2) A series of values are chosen for ϵ_{xp}. For each of these values,

(a) Compute ϵ_{ep} from equations (B5).

(b) Read σ_e from the stress-strain curve.

(c) Compute $\epsilon_x - \alpha T$ and $\epsilon_\theta - \alpha T$ from equations (D3). Thus, one curve of the family is obtained.

(3) To obtain the other curves, new values are chosen for $\epsilon_{\theta p}$, and the process is repeated in each case.

The limiting curve of zero plastic strain is an ellipse about the origin as shown in figure 4. Any point inside this ellipse corresponds to zero plastic strain.

APPENDIX E

LONG SOLID CYLINDER

Consider an infinitely long circular cylinder which has a radial temperature distribution $T(r)$. The equilibrium equation is

$$\frac{d\sigma_r}{dr} + \frac{\sigma_r - \sigma_\theta}{r} = 0 \tag{E1}$$

The compatibility relation is

$$\epsilon_r - \epsilon_\theta = r \frac{d\epsilon_\theta}{dr} \tag{E2}$$

Substituting equations (29) into (E1), assuming E constant, and eliminating ϵ_r by use of equation (E2) give

$$\frac{d}{dr}\left[\frac{1}{r}\frac{d}{dr}(r^2\epsilon_\theta)\right] = \frac{1+\nu}{1-\nu}\alpha\frac{dT}{dr} + \frac{1-2\nu}{1-\nu}\frac{1}{r}\frac{d}{dr}(r\epsilon_{rp}) - \frac{1-2\nu}{1-\nu}\frac{\epsilon_{\theta p}}{r} \tag{E3}$$

Integrating equation (E3) results in

$$\epsilon_\theta = \frac{1+\nu}{1-\nu}\frac{1}{r^2}\int_0^r \alpha T r\, dr + \frac{1-2\nu}{1-\nu}\frac{1}{r^2}\int_0^r \epsilon_{rp} r\, dr + \frac{1-2\nu}{1-\nu}\frac{1}{r^2}\int_0^r r\int_0^r \frac{\epsilon_{rp} - \epsilon_{\theta p}}{r}\, dr\, dr + C_1 + \frac{C_2}{r^2} \tag{E4}$$

For a solid cylinder C_2 must equal zero. Also, equation (E2) can be rewritten as

$$\epsilon_r = -\epsilon_\theta + \frac{1}{r}\frac{d}{dr}(r^2\epsilon_\theta) \tag{E5}$$

By using equation (E3), equation (E5) can be written as:

$$\epsilon_r = -\epsilon_\theta + \frac{1+\nu}{1-\nu}\alpha T + \frac{1-2\nu}{1-\nu}\epsilon_{rp} + \frac{1-2\nu}{1-\nu}\int_0^r \frac{\epsilon_{rp} - \epsilon_{\theta p}}{r}\, dr + 2C_1 \tag{E6}$$

To determine ϵ_z, use is made of the fact that ϵ_z is a constant and that

$$\int_0^R \sigma_z r \, dr = 0 \tag{E7}$$

Substituting the last of equations (29) into (E7) and using equations (E4) and (E6) enables ϵ_z to be determined. To obtain C_1, the surface boundary condition $\sigma_r(R) = 0$ is used. Substituting the first of equations (29) into this relation enables C_1 to be calculated. The final results are given in equations (28).

APPENDIX F

ROTATING DISK

The derivation of the equations for the rotating disk with a radial temperature distribution is very similar to the derivations of the equations for the long solid cylinder (appendix E). For the disk problem, the axial stress σ_z is assumed to be zero, and the axial strain ϵ_z is no longer a constant. The equilibrium equation for this case is

$$\frac{d}{dr}(hr\sigma_r) - h\sigma_\theta + \rho\omega^2 hr^2 = 0 \tag{F1}$$

The compatibility equation is the same as equation (E2), and the stress-strain relations with σ_z equal to zero become

$$\left.\begin{aligned}\sigma_r &= \frac{E}{1-\nu^2}\left[\epsilon_r + \nu\epsilon_\theta - (\epsilon_{rp} + \nu\epsilon_{\theta p}) - (1+\nu)\alpha T\right] \\ \sigma_\theta &= \frac{E}{1-\nu^2}\left[\epsilon_\theta + \nu\epsilon_r - (\epsilon_{\theta p} + \nu\epsilon_{rp}) - (1+\nu)\alpha T\right]\end{aligned}\right\} \tag{F2}$$

For a parallel-sided disk with E assumed constant, the solution is readily obtained. Substituting equations (F2) into (F1) and using equation (E2) result in

$$\frac{d}{dr}\left[\frac{1}{r}\frac{d}{dr}(r^2\epsilon_\theta)\right] = -\frac{1-\nu^2}{E}\rho\omega^2 r + (1+\nu)\frac{d(\alpha T)}{dr} + \frac{d}{dr}(\epsilon_{rp} + \nu\epsilon_{\theta p}) + (1-\nu)\frac{\epsilon_{rp} - \epsilon_{\theta p}}{r} \tag{F3}$$

and, after integrating,

$$\epsilon_\theta = -\frac{(1-\nu^2)}{E}\frac{\rho\omega^2 r^2}{8} + \frac{1+\nu}{r^2}\int_0^r \alpha T r\,dr + \frac{1-\nu}{2}\int_0^r \frac{\epsilon_{rp} - \epsilon_{\theta p}}{r}\,dr + \frac{1+\nu}{2r^2}\int_0^r r(\epsilon_{rp} + \epsilon_{\theta p})dr + \frac{C_3}{2} + \frac{C_4}{r^2} \tag{F4}$$

where for a solid disk C_4 must vanish. To obtain ϵ_r, equation (F4) is substituted into equation (E2) resulting in

$$\epsilon_r = -\epsilon_\theta - \frac{1 - \nu^2}{E}\frac{\rho\omega^2 r^2}{2} + (1 + \nu)\alpha T + \epsilon_{rp} + \nu\epsilon_{\theta p} + (1 - \nu)\int_0^r \frac{\epsilon_{rp} - \epsilon_{\theta p}}{r}\,dr + C_3 \qquad \text{(F5)}$$

The term ϵ_z can now be computed from equations (B2) with σ_z taken as zero. Thus,

$$\epsilon_z = -\frac{\nu}{1 - \nu}(\epsilon_r + \epsilon_\theta) - \frac{1 - 2\nu}{1 - \nu}(\epsilon_{rp} + \epsilon_{\theta p}) + \frac{1 + \nu}{1 - \nu}\alpha T \qquad \text{(F6)}$$

The constant C_3 is evaluated from the known rim loading. If the rim stress due to the rim loading is $\sigma_r(R)$, the first of equations (F2) becomes

$$\sigma_r(R) = \frac{E}{1 - \nu^2}\left[\epsilon_r + \nu\epsilon_\theta + (\epsilon_{rp} + \nu\epsilon_{\theta p}) - (1 + \nu)\alpha T\right]_{r=R} \qquad \text{(F7)}$$

Substituting equations (F4) and (F5) into equation (F7) enables C_3 to be calculated. The final equations are given in equations (30).

APPENDIX G

EFFECT OF PREVIOUS PLASTIC STRAIN

If the body under consideration has undergone previous plastic strain such as that during a thermal shock in which the stresses and the plastic deformations vary with time, a complete series of solutions must be carried out for successive time intervals. The equations for the strains remain the same except that each plastic strain term such as ϵ_{rp} is replaced by $\Sigma\epsilon_{rp} + \Delta\epsilon_{rp}$, where $\Sigma\epsilon_{rp}$ is the total accumulated plastic strain up to the previous time and $\Delta\epsilon_{rp}$ is the additional plastic strain during the time interval under consideration. These strains $\Sigma\epsilon_{rp}$ and $\Sigma\epsilon_{\theta p}$ are known from the previous calculations, and the total strain equations are solved by successive approximation to obtain the change in plastic strains $\Delta\epsilon_{rp}$ and $\Delta\epsilon_{\theta p}$ as well as the total strains after the new time interval.

In carrying out this type of calculation for successive time intervals, a time may eventually be reached when some point in the body begins to unload, that is, σ_e starts decreasing. When this time is reached, no additional plastic flow will take place at this point, and unloading will proceed along an elastic line such as CC' in figure 1. At this station then, the plastic strains are assumed to be zero from this time on. The successive approximations are continued in the usual manner until all points in the cylinder begin to unload or equilibrium conditions are reached.

This type of procedure of adding the plastic flow occurring after each time increment to the previously accumulated plastic flow is equivalent to the assumption that, as the load and temperature change, the stress position on the new stress-strain curve would be the same as if a test specimen were loaded above the yield point, the load removed, the temperature changed, and a new load applied. This assumption is illustrated in figure 11 in which point A represents a loading at the first temperature conditions; the dotted line AB represents the unloading path; the curve BCD shows the stress-strain curve at the new temperature; and point C gives the new stress position. The total strain at this point C is given by the sum of three strains: the residual strain caused by the first loading, the elastic part of the strain caused by the second loading, and the plastic strain caused by the second loading.

When the foregoing procedure is applied, the curve BCD must, of course, represent the true stress-strain curve at the new temperature of a material that has already been subjected to the plastic cycle OAB. In general, this new stress-strain curve is different from the stress-strain

curve at the given temperature of a material that has not been subjected to plastic flow. However, unless data are available, it may be necessary to assume that the curve BCD is the stress-strain curve at the given temperature of a specimen of virgin material. Results obtained in this way, however, should be treated cautiously since this effect may be appreciable.

REFERENCES

1. Ilyushin, A. A.: Some Problems in the Theory of Plastic Deformations. BMB-12, trans. by Grad. Div. Appl. Math., Brown Univ., for David W. Taylor Model Basin, 1946. (Contract NObs-34166.)

2. Ince, E. L.: Ordinary Differential Equations. Dover Pub., 1944.

3. Manson, S. S.: Analysis of Rotating Disks of Arbitrary Contour and Radial Temperature Distribution in the Region of Plastic Deformation. Proc. First U.S. Nat. Cong. Appl. Mech., ASME, 1952, pp. 569-577.

4. Wang, Chi-Teh: Applied Elasticity. McGraw-Hill Book Co., Inc., 1953.

TABLE I. - PLASTIC FLOW CALCULATIONS

(a) Flat plate

Station	y	ϵ_{ep}	ϵ (Eq. (13))	ϵ_{ep} (Fig. 1)	ϵ (Eq. (13))	ϵ_{ep} (Fig. 1)	ϵ (Eq. (13))	ϵ_{ep} (Fig. 1)	ϵ (Eq. (13))	ϵ_{ep} (Fig. 1)	ϵ (Eq. (13))	ϵ_{ep} (Fig. 1)
1	0	0	1.9×10^{-3}	0.7×10^{-3}	1.7×10^{-3}	0.5×10^{-3}	1.6×10^{-3}	0.4×10^{-3}	1.6×10^{-3}	0.4×10^{-3}	1.6×10^{-3}	0.4×10^{-3}
2	.1	0	1.8	.6	1.6	.4	1.5	.4	1.5	.4	1.5	.4
3	.2	0	1.7	.5	1.5	.4	1.4	.3	1.4	.3	1.4	.3
4	.3	0	1.4	.3	1.2	.2	1.1	.1	1.1	.1	1.1	.1
5	.4	0	1.0	0	.8	0	.7	0	.7	0	.7	0
6	.5	0	.5	0	.3	0	.2	0	.2	0	.2	0
7	.6	0	-.2	0	-.4	0	-.4	0	-.5	0	-.5	0
8	.7	0	-.9	0	-1.1	-.1	-1.2	-.2	-1.2	-.2	-1.2	-.2
9	.8	0	-1.7	-.5	-1.9	-.7	-2.0	-.8	-2.0	-.8	-2.0	-.8
10	.9	0	-2.7	-1.5	-2.9	-1.6	-3.0	-1.7	-3.0	-1.7	-3.0	-1.7
11	1.0	0	-3.8	-2.5	-4.0	-2.7	-4.0	-2.7	-4.1	-2.8	-4.1	-2.8

(b) Thin shell

CS-13076

Station	x	z	αT	ϵ_{xp} (Previous approximation)	$\epsilon_{\theta p}$ (Previous approximation)	I_1 (Previous approximation)	I_2 (Previous approximation)	w (Eq. (23))	$\epsilon_x - \alpha T$ (Eq. (18))	$\epsilon_\theta - \alpha T$ (Eq. (18))	ϵ_{xp} (Fig. 5)	$\epsilon_{\theta p}$ (Fig. 5)	Q (Eq. (22))	P (Eq. (22))	I_1 (Eq. (24))	I_2 (Eq. (24))	w
20	11.97	-1.0	-5.008×10^{-3}	0.850×10^{-3}	-0.800×10^{-3}	-64.14×10^{-6}	-581.1×10^{-6}	-0.01572	1.314×10^{-3}	-1.865×10^{-3}	0.800×10^{-3}	-0.785×10^{-3}	-0.03295	-0.008013	-82.55×10^{-6}	-545.6×10^{-6}	-0.01414
		-.6667		.480	-.770				1.110		.505	-.745					
		-.3333		.420	-.740				.9100		.420	-.705					
		0		.385	-.725				.7088		.340	-.670					
		.3333		.310	-.710				.5100		.270	-.650					
		.6667		.260	-.700				.3100		.200	-.640					
		1.0		.215	-.695				.1000		.155	-.650					
21	12.60	-1.0	-3.333	-3.20	-2.500	-1115	-1952	0	-4.414	-3.335	-3.350	-2.500	-0.1150	0.06150	-1045	-2185	0
		-.6667		-1.57	-2.270				-2.490		-1.625	-2.280					
		-.3333		-.175	-2.075				-.5700		-.175	-2.075					
		0		.840	-2.050				1.348		.995	-2.050					
		.3333		2.170	-2.300				3.270		2.355	-2.325					
		.6667		3.600	-2.750				5.190		4.000	-2.755					
		1.0		5.500	-2.850				7.110		5.800	-2.850					

[a] In calculating w, σ_θ and σ_i are calculated from eq. (21) by using eqs. (25) and (26).

TABLE I. - Concluded. PLASTIC FLOW CALCULATIONS

(c) Long solid cylinder

Station	r	αT	ε_{rp} (Previous approximation)	$\varepsilon_{\theta p}$ (Previous approximation)	ε_r (Eq. (28))	ε_θ (Eq. (28))	ε_z (Eq. (28))	ε_{et} (Eq. (3))	ε_{ep} (Fig. 2)	ε_{rp} (Eq. (4))	$\varepsilon_{\theta p}$ (Eq. (4))
1	0	9.50×10^{-3}	0	0	9.457×10^{-3}	9.457×10^{-3}	8.912×10^{-3}	0.363×10^{-3}	0×10^{-3}	0×10^{-3}	0×10^{-3}
2	.75	9.50	0	0	9.462	9.452	0	.363	0	0	0
3	.80	9.29	0	0	9.085	9.439	0	.310	0	0	0
4	.85	8.81	0	0	8.240	9.393	0	.668	0	0	0
5	.90	7.68	0	0	6.236	9.299	0	1.926	0.91	-.907	0.545
6	.95	7.06	0	0	5.274	9.109	0	2.494	1.40	-1.397	.754
7	1.000	6.83	0	0	5.045	8.911	0	2.578	1.48	-1.477	.738

CS-13078

(d) Rotating disk

Station	r	αT	ε_{rp} (Previous approximation)	$\varepsilon_{\theta p}$ (Previous approximation)	ε_r (Eq. (30))	ε_θ (Eq. (30))	ε_z (Eq. (30))	ε_{et} (Eq. (3))	ε_{ep} (Fig. 2)	ε_{rp} (Eq. (4))	$\varepsilon_{\theta p}$ (Eq. (4))
1	0	0.95×10^{-3}	1.567×10^{-3}	1.567×10^{-3}	3.757×10^{-3}	3.757×10^{-3}	-3.247×10^{-3}	4.669×10^{-3}	3.441×10^{-3}	1.720×10^{-3}	1.720×10^{-3}
2	.5	1.045	1.515	1.517	3.780	3.784	-3.033	4.543	3.317	1.657	1.680
3	1.0	1.33	1.459	1.351	3.983	3.845	-2.490	4.270	3.048	1.573	1.474
4	1.5	1.71	1.376	1.144	4.250	3.942	-1.776	3.919	2.721	1.466	1.252
5	2.0	2.47	1.256	.7269	4.862	4.104	-.3885	3.277	2.124	1.298	.8067
6	2.5	3.80	1.089	.1111	6.022	4.381	1.913	2.389	1.304	1.047	.1508
7	3.0	5.415	1.070	-.4288	7.614	4.797	4.371	2.035	.9972	.9899	-.3908
8	3.5	7.315	1.410	-1.175	9.773	5.362	6.964	2.578	1.469	1.371	-1.142
9	4.0	9.5	1.904	-2.298	12.28	6.076	10.00	3.623	2.446	1.908	-2.279
10	4.5	11.88	2.290	-3.637	14.83	6.911	13.51	4.896	3.664	2.303	-3.620
11	5.0	14.25	2.498	-4.996	17.18	7.824	17.18	6.235	4.982	2.491	-4.982

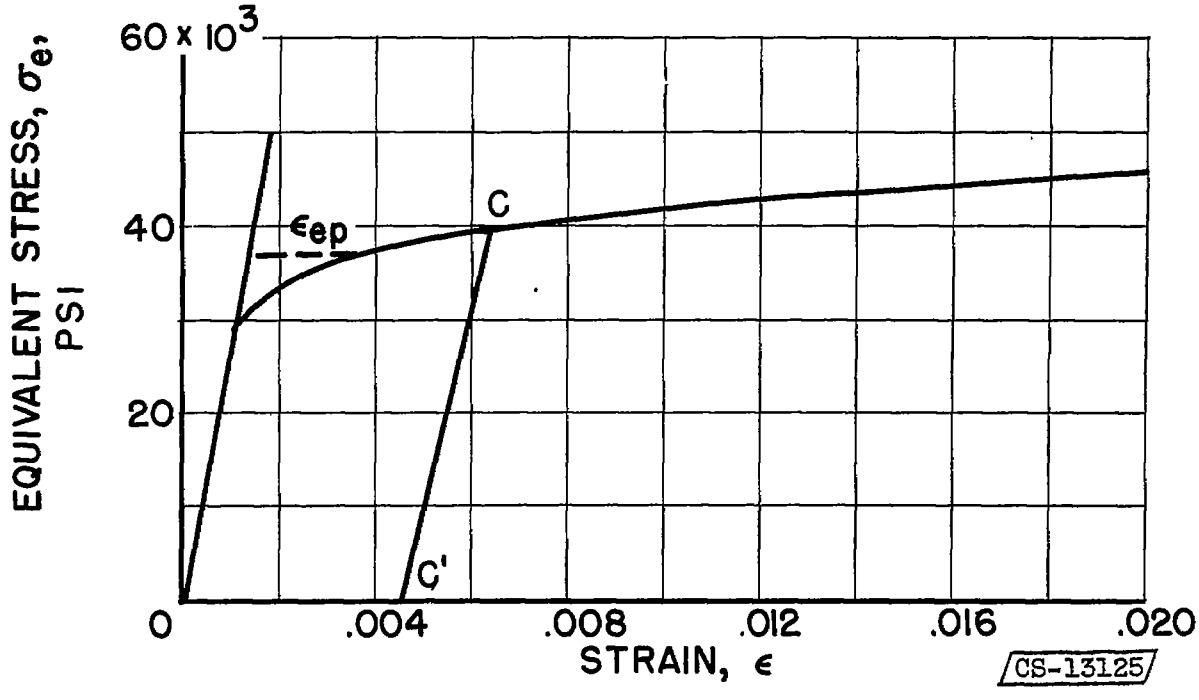

Figure 1. - Typical stress-strain curve for 18-8 stainless steel.

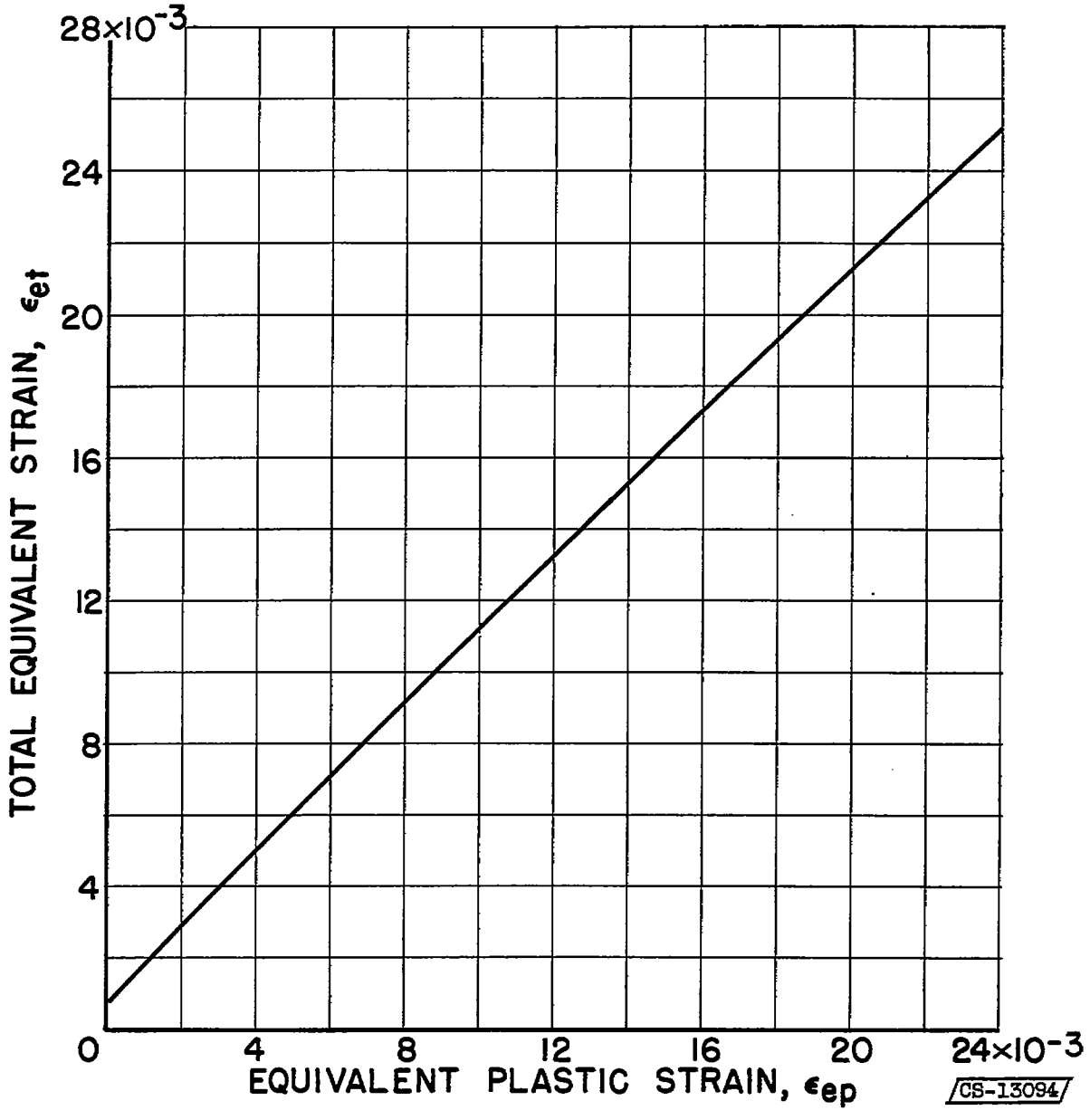

Figure 2. - Variation of total equivalent strain with equivalent plastic strain based on stress-strain curve of figure 1.

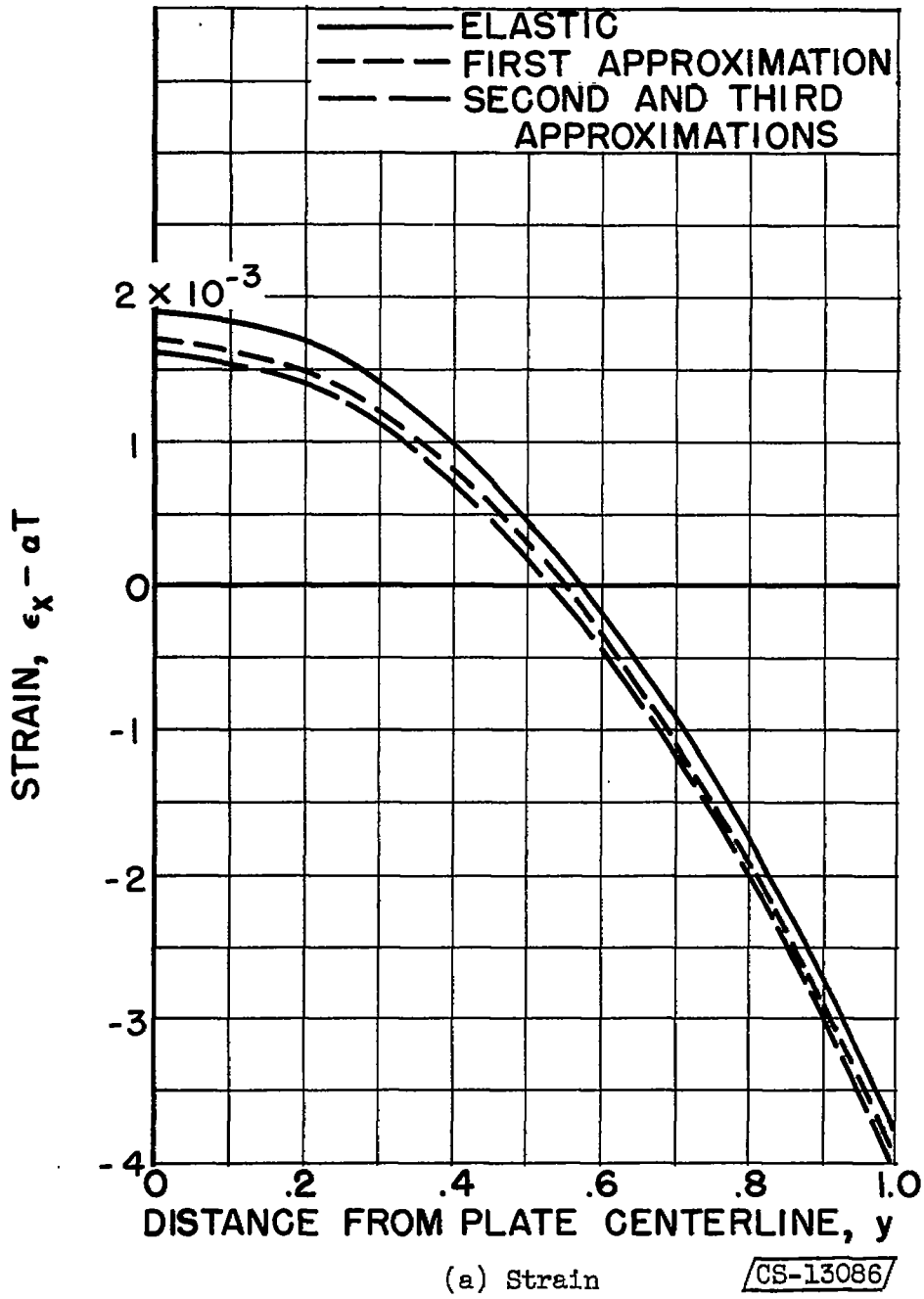

(a) Strain

Figure 3. - Variation of stress and strain along flat plate for successive approximations. Temperature given by $T = 600(y^2 - \frac{1}{3}) + T_0$.

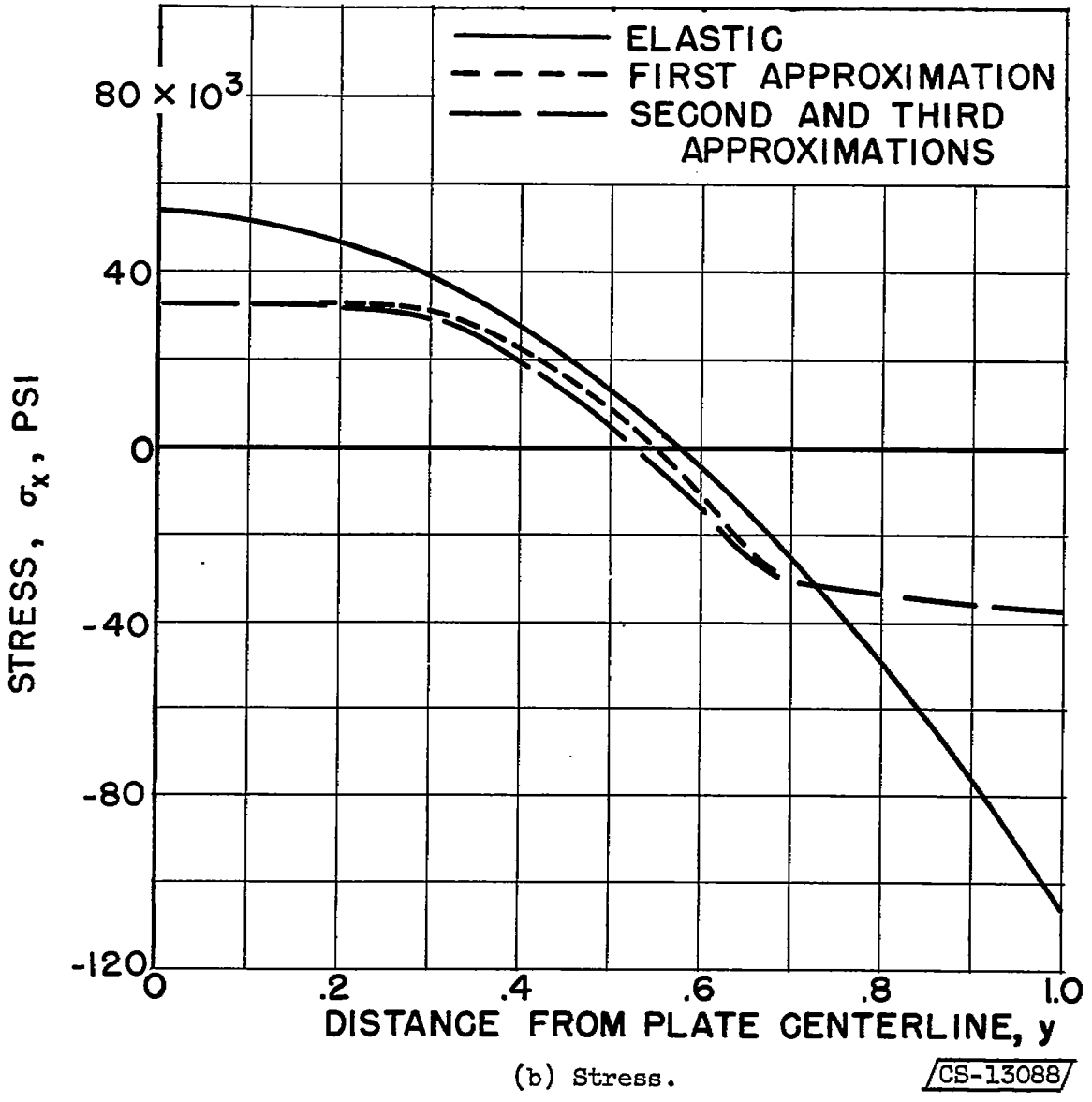

(b) Stress.

Figure 3. - Concluded. Variation of stress and strain along flat plate for successive approximations. Temperature given by $T = 600(y^2 - \frac{1}{3}) + T_0$.

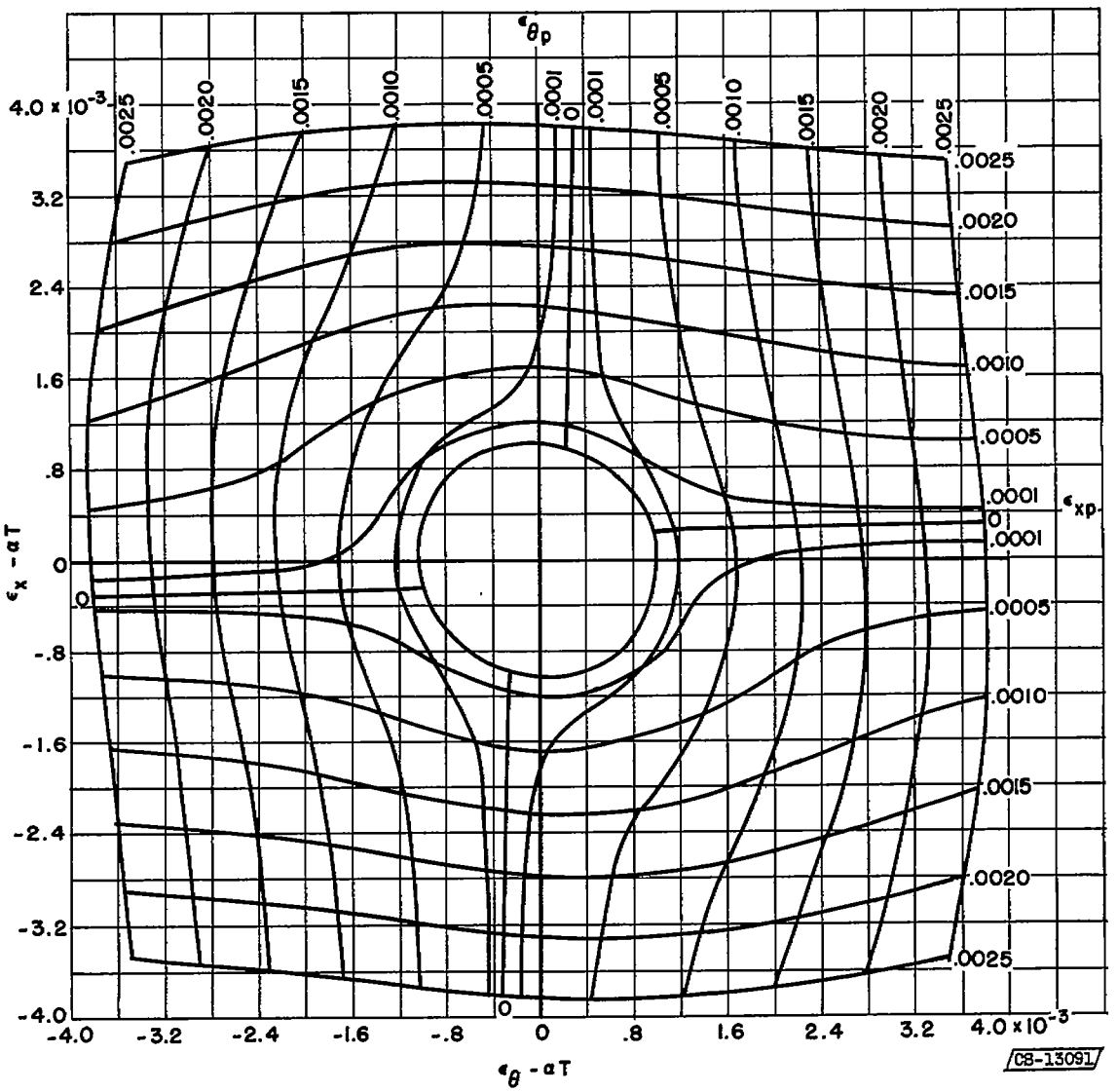

Figure 4. - Plastic strain chart based on stress-strain curve of figure 1.

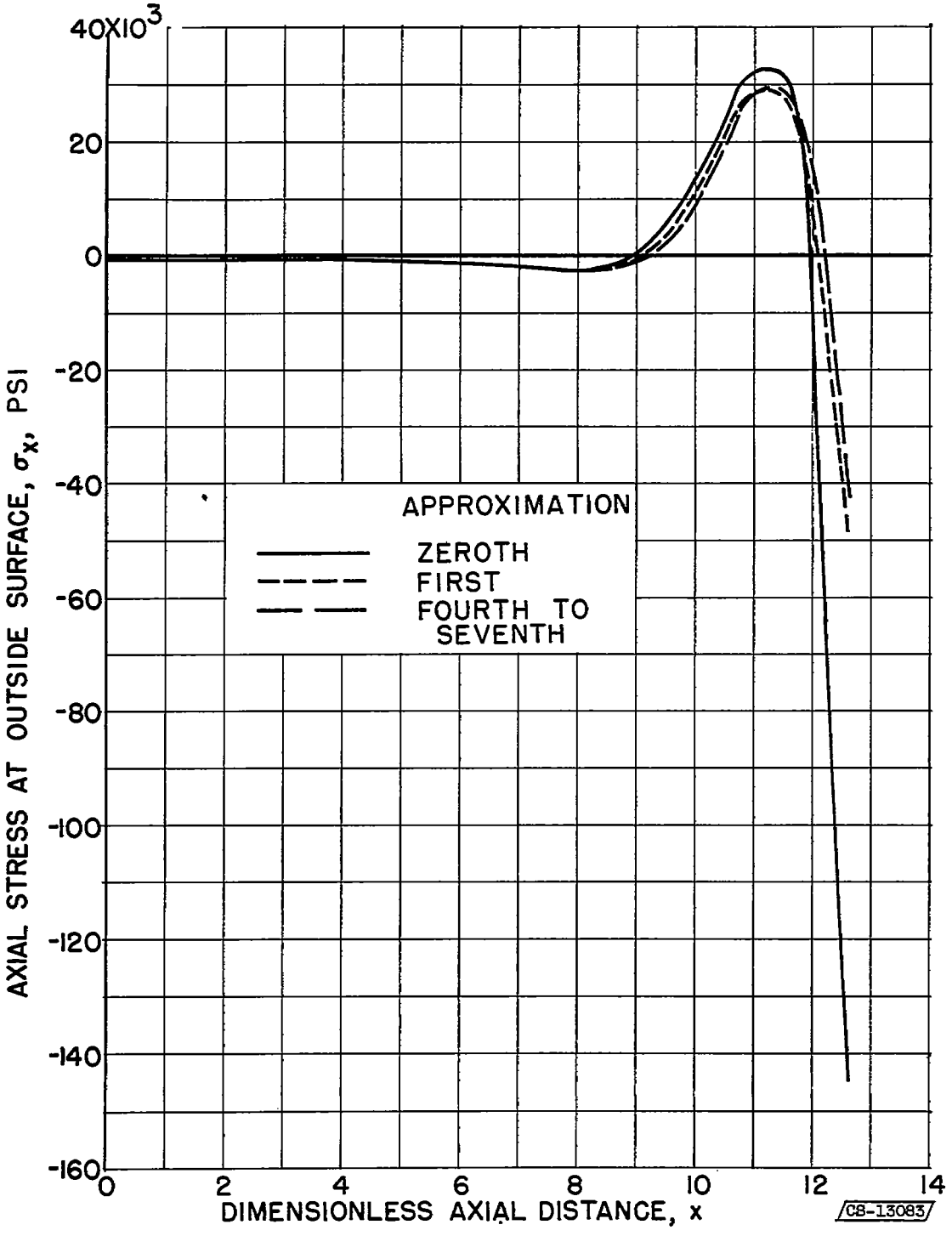

(a) Axial stress on outside surface of thin shell.

Figure 5. - Variation of stresses and strains on shell with axial distance measured in terms of characteristic length. Temperature distribution, $T = 2.21x^2$.

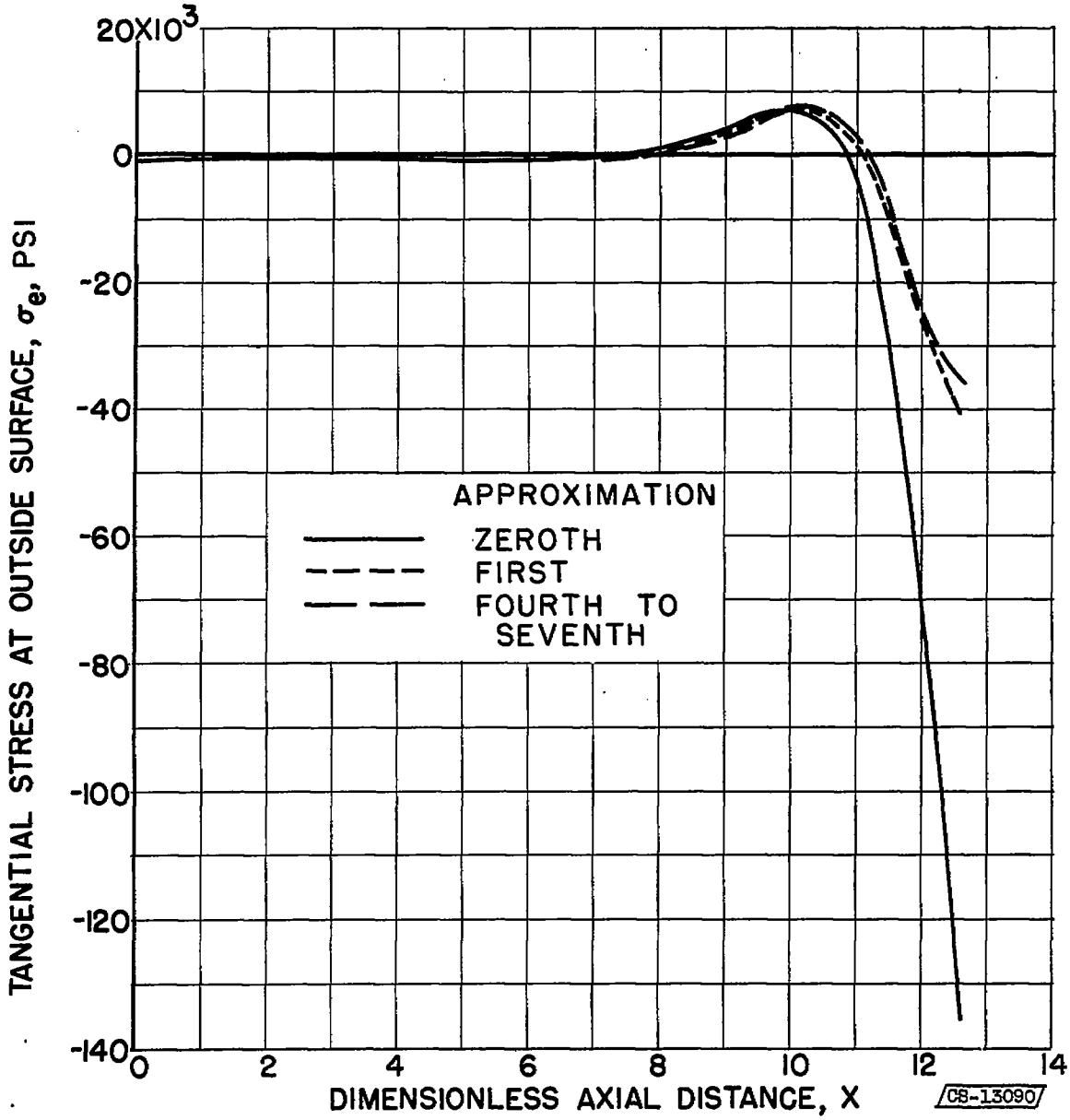

(b) Tangential stress on outside surface of shell.

Figure 5. - Continued. Variation of stresses and strains on shell with axial distance measured in terms of characteristic length. Temperature distribution, $T = 2.21x^2$.

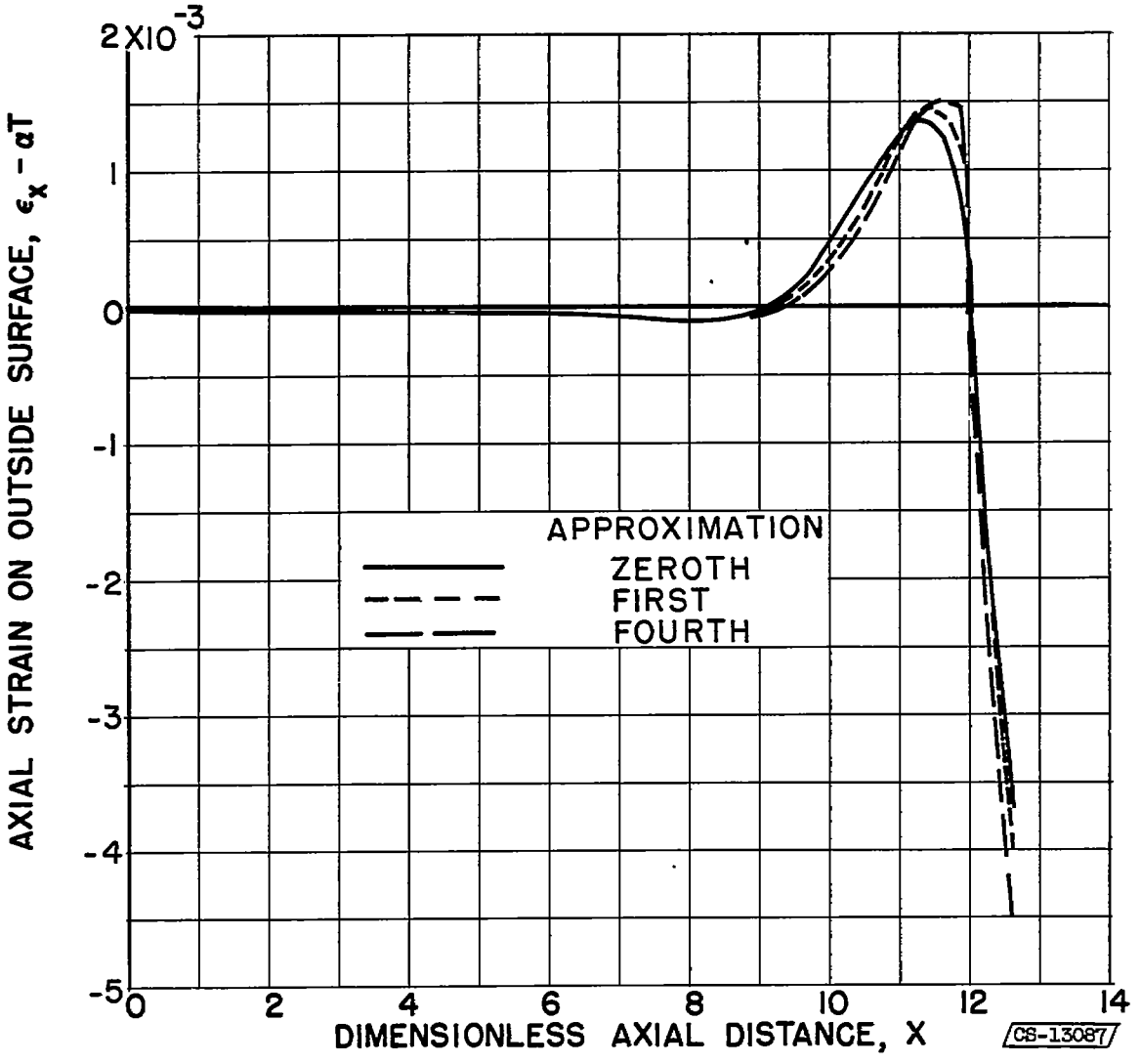

(c) Axial strain on outside surface of thin shell.

Figure 5. - Continued. Variation of stresses and strains on shell with axial distance measured in terms of characteristic length. Temperature distribution, $T = 2.21x^2$.

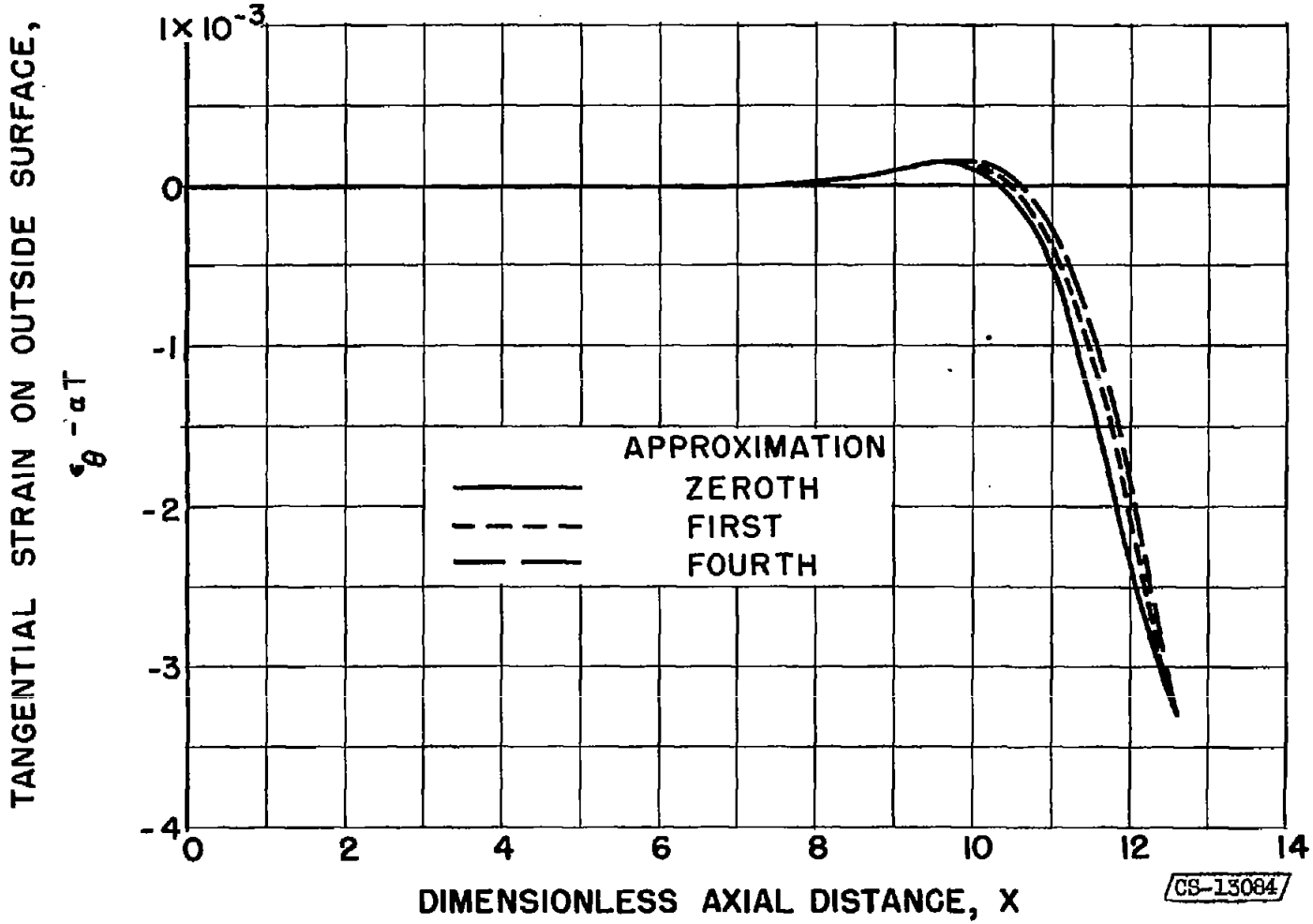

(d) Tangential strain on outside surface of shell.

Figure 5. - Concluded. Variation of stresses and strains on shell with axial distance measured in terms of characteristic length. Temperature distribution, $T = 2.21x^2$.

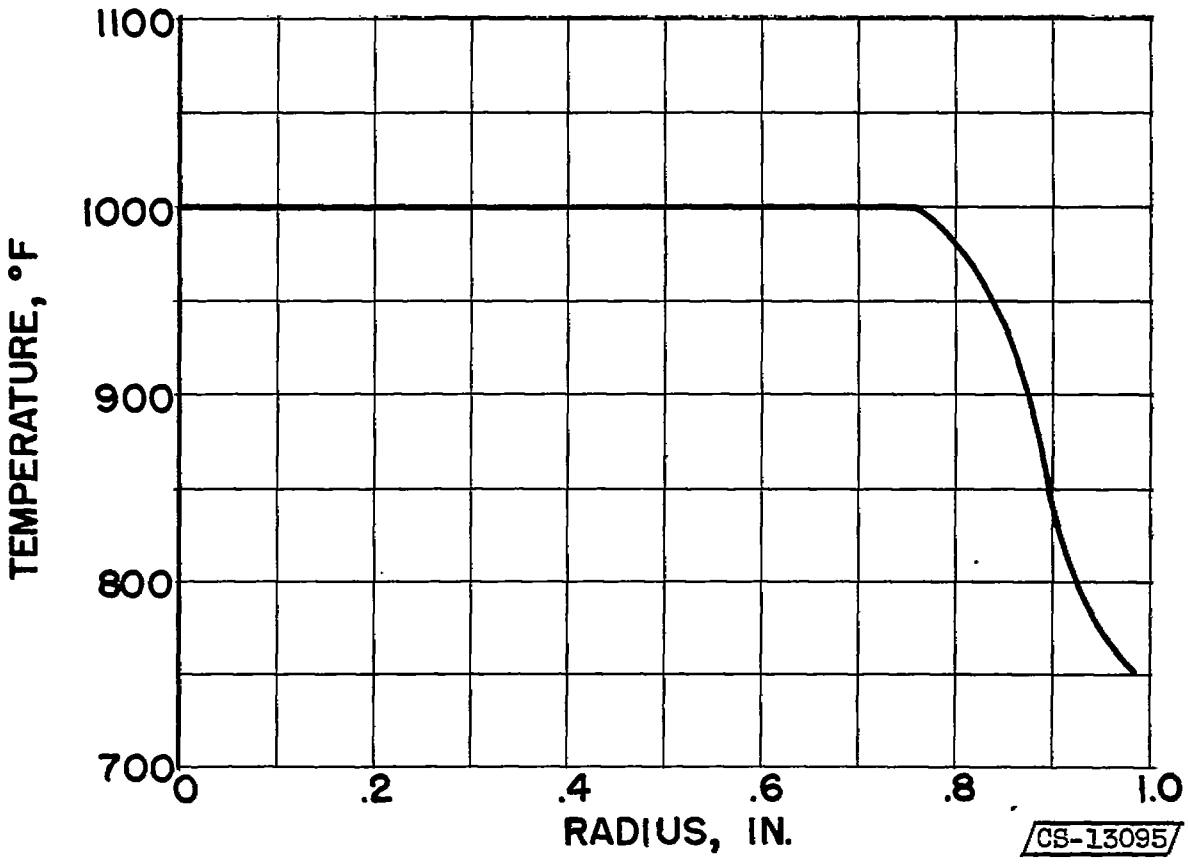

Figure 6. - Radial temperature distribution in long solid cylinder.

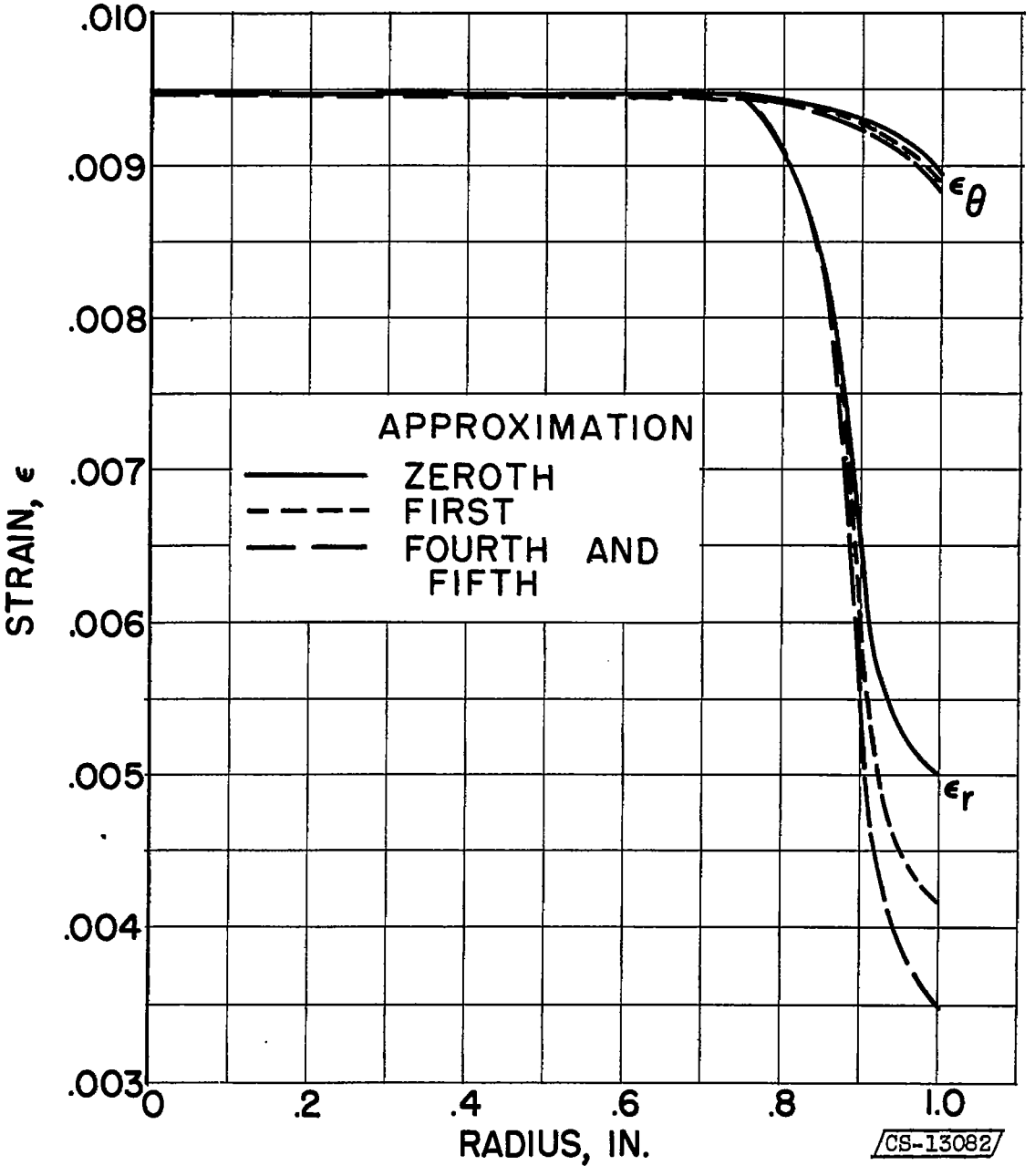

(a) Strain.

Figure 7. - Strain and stress distributions in long solid cylinder with radial temperature gradient.

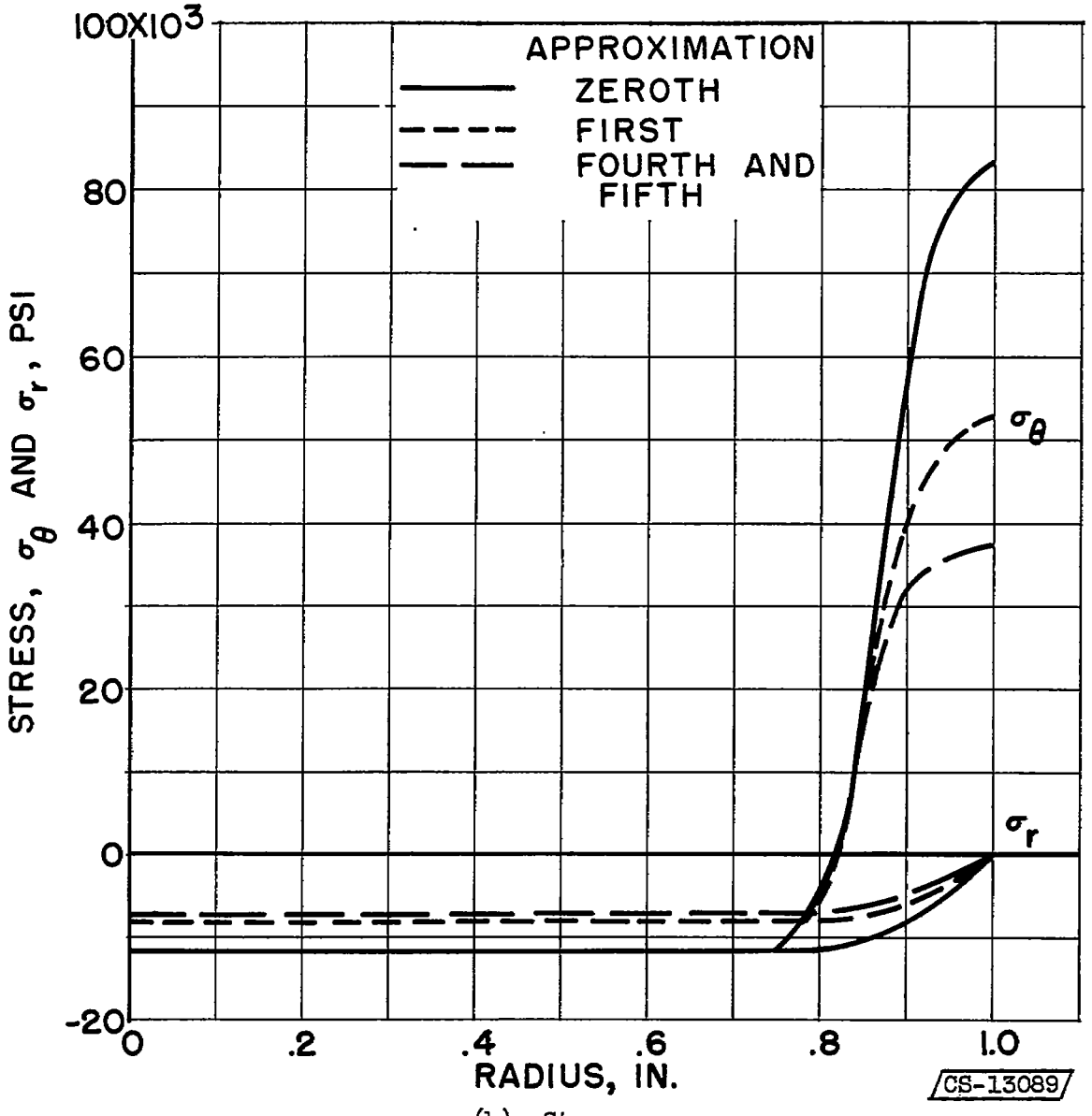

(b) Stress.

Figure 7. - Concluded. Strain and stress distributions in long solid cylinder with radial temperature distribution.

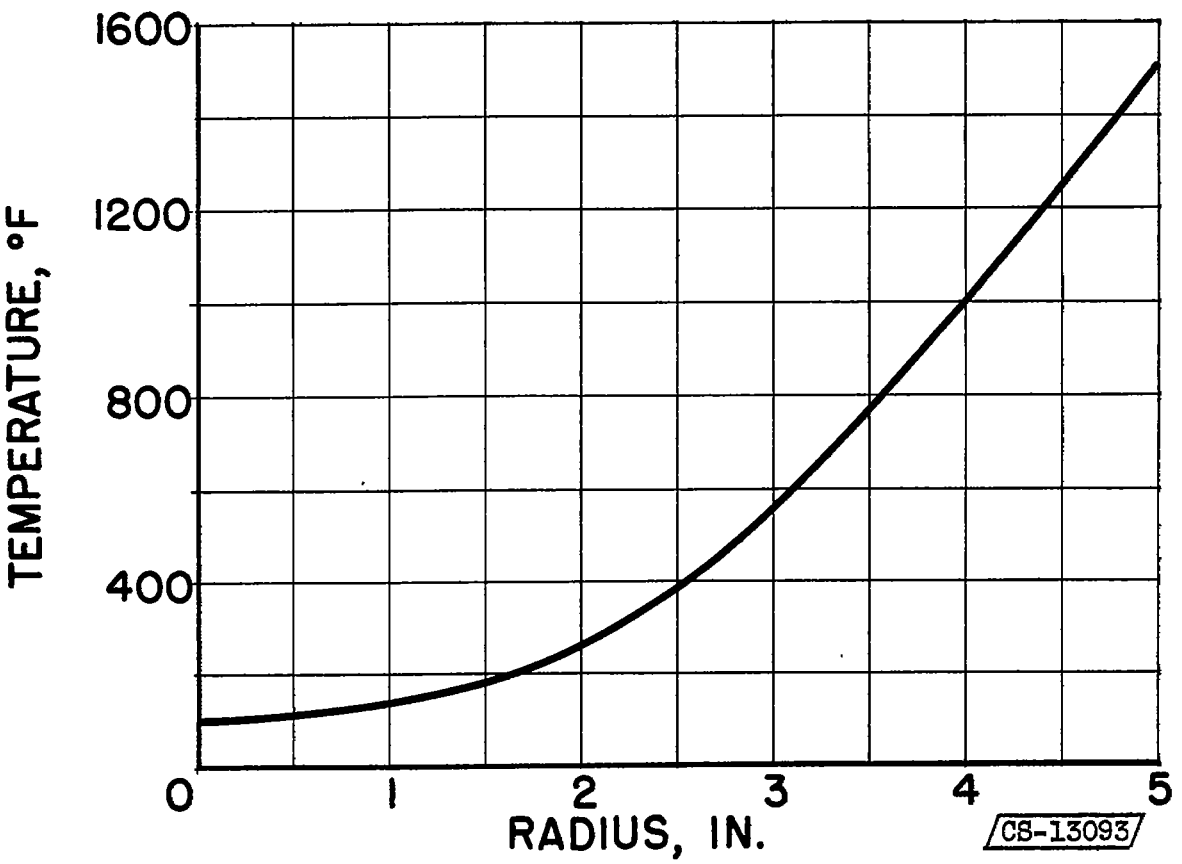

Figure 8. - Temperature distribution in rotating disk.

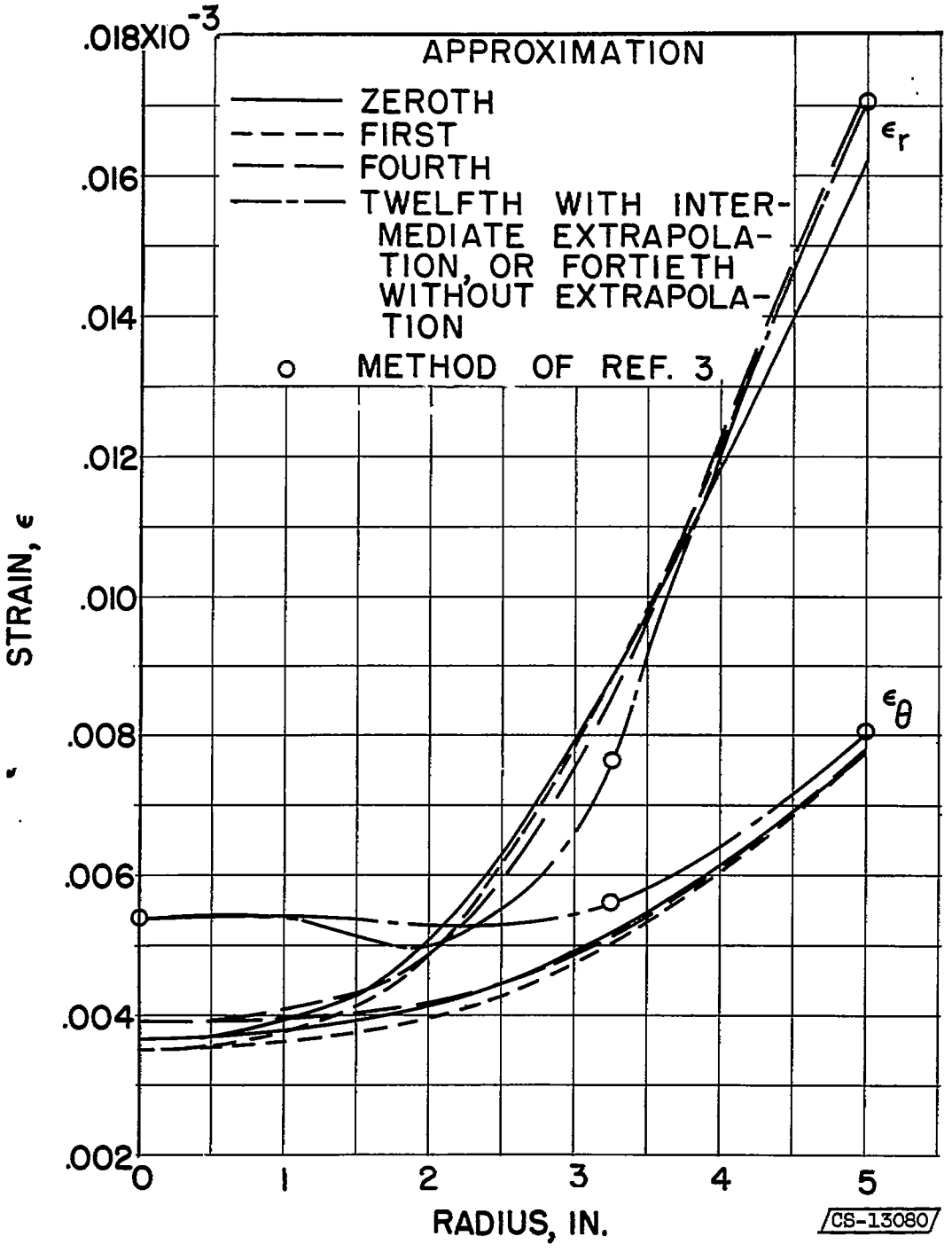

(a) Strain.

Figure 9. - Strain and stregs distributions in rotating disk with temperature gradient. $\rho\omega^2 = 1500$.

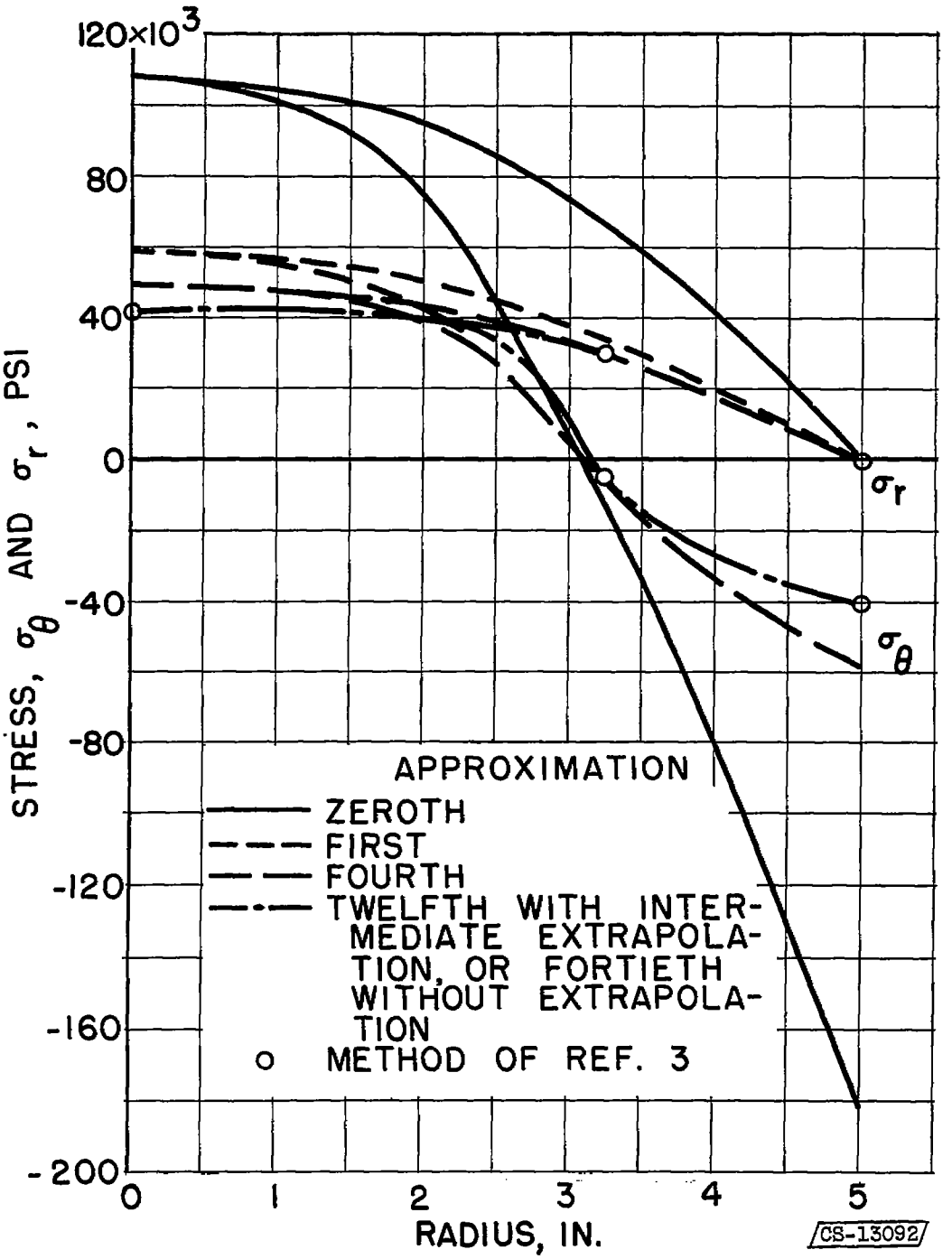

(b) Stress.

Figure 9. - Concluded. Strain and stress distributions in rotating disk with temperature gradient. $\rho\omega^2 = 1500$.

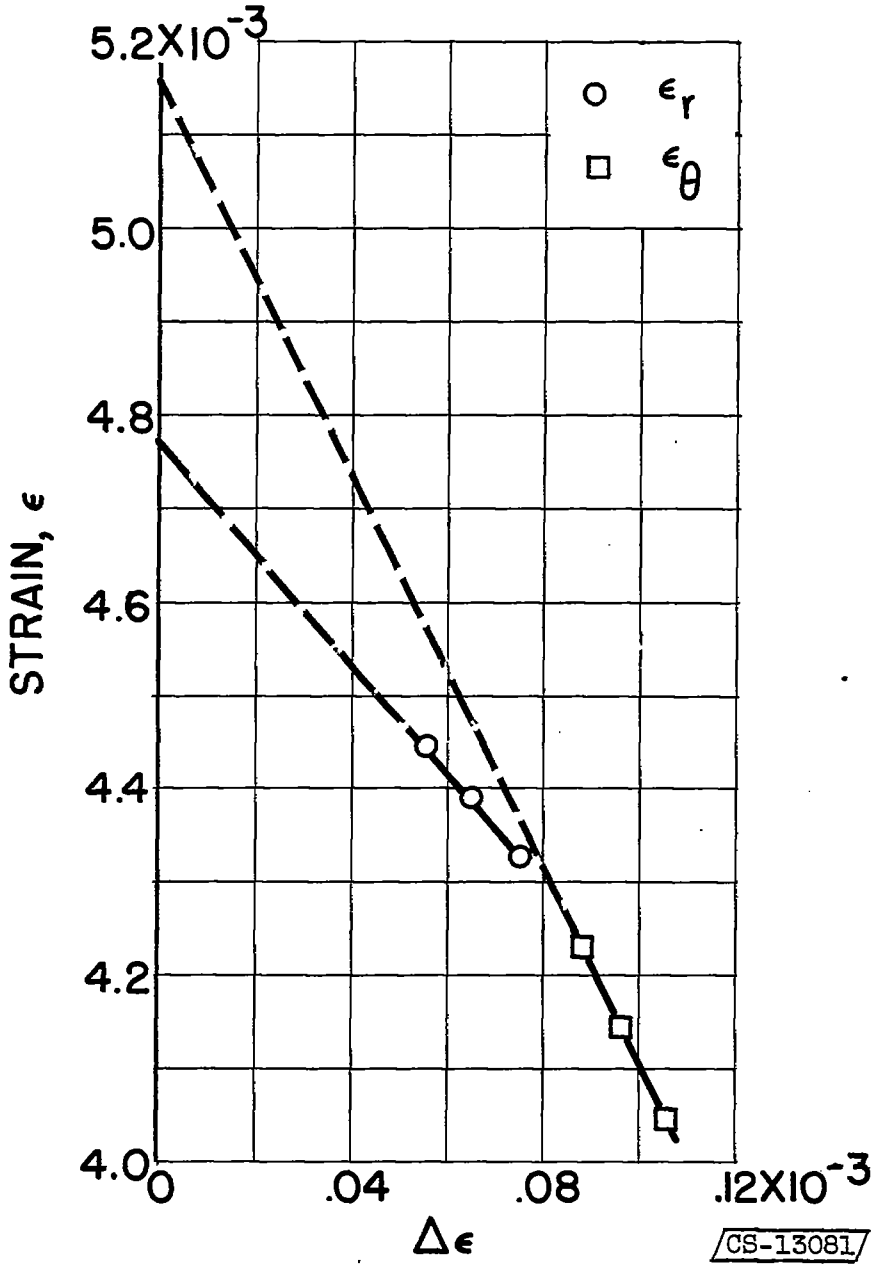

Figure 10. - Variation of strain with change of strain for four successive approximations for rotating disk with temperature gradient.

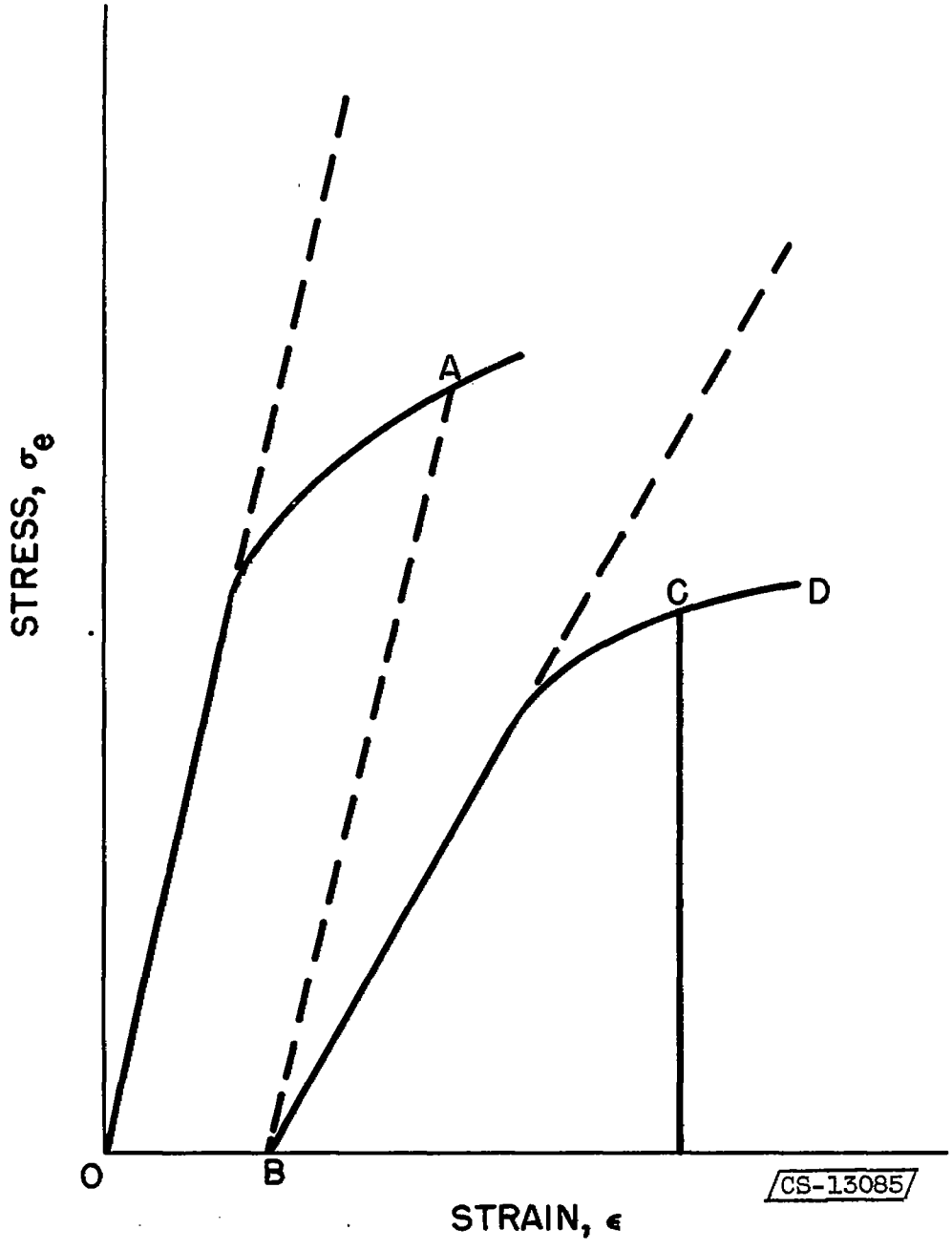

Figure 11. - Uniaxial stress-strain curves showing components of strain when plastic flow occurs a second time.